JCTC Journal of Chemical Theory and Computation

Article

pubs.acs.org/JCTC

Correlated Ab Initio and Density Functional Studies on H_2 Activation by FeO^+

Ahmet Altun,[†] Jürgen Breidung,[‡] Frank Neese,[§] and Walter Thiel*[,‡]

[†]Department of Physics, Fatih University, 34500 B.Çekmece, Istanbul, Turkey

[‡]Max-Planck-Institut für Kohlenforschung, Kaiser-Wilhelm-Platz 1, D-45470 Mülheim an der Ruhr, Germany

[§]Max-Planck-Institut für Chemische Energiekonversion, Stiftstr. 34-36, D-45470 Mülheim an der Ruhr, Germany

Supporting Information

ABSTRACT: The reaction $FeO^+ + H_2 \rightarrow Fe^+ + H_2O$ is a simple model for hydrogen abstraction processes in biologically important heme systems. The geometries of all relevant stationary points on the lowest sextet and quartet surfaces were optimized using several density functionals as well as the CASSCF method. The corresponding energy profiles were computed at the following levels: density functional theory using gradient-corrected, hybrid, meta, hybrid-meta, and perturbatively corrected double hybrid functionals; single-reference coupled cluster theory including up to single, double, triple, and perturbative quadruple excitations [CCSDT(Q)]; correlated multireference ab initio methods (MRCI, MRAQCC, SORCI, SORCP, MRMP2, NEVPT2, and CASPT2). The calculated energies were corrected for scalar relativistic effects, zero-point vibrational energies, and core−valence correlation effects. MRCI and SORCI energies were corrected for size-consistency errors using an a posteriori Davidson correction (+Q) leading to MRCI+Q and SORCI+Q. Comparison with the available experimental data shows that CCSDT(Q) is most accurate and can thus serve as benchmark method for this electronically challenging reaction. Among the density functionals, B3LYP performs best. In the correlated ab initio calculations with a full-valence active space, SORCI+Q yields the lowest deviations from the CCSDT(Q) reference results, with qualitatively similar energy profiles being obtained from MRCI+Q and MRAQCC. SORCI+Q benefits from the quality of the approximate average natural orbitals used in the final step of the SORCI procedure. Many of the tested methods show surprisingly large errors. The present results validate the common use of B3LYP in computational studies of heme systems and offer guidance on which correlated ab initio methods are most suitable for such studies.

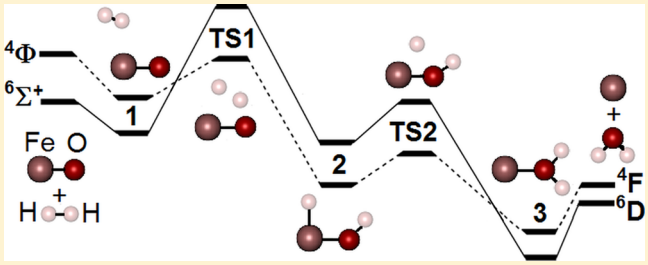

INTRODUCTION

The activation of inert saturated bonds is of great importance in chemistry.[1,2] Several heme and nonheme metalloenzymes that contain FeO moieties in various oxidation and spin states are efficient catalysts for such reactions, which often involve an initial hydrogen abstraction step.[3−14] Extensive experimental and theoretical studies have been performed on these catalytic reactions.[3−14]

Density functional theory (DFT) has often been applied with great success to transition metal compounds.[3−8] DFT methods normally provide reasonable structures and relative energies of stable molecules but are regarded as less reliable for reaction barriers.[3−8,15−19] As an example, we consider the simplest hydrogen abstraction reaction, $H_2 + H \rightarrow [H\cdots H\cdots H]^{\ddagger} \rightarrow H + H_2$. When using the 6-311++G(3df,3pd) basis, coupled cluster CCSD(T) calculations yield a reference barrier of 9.9 kcal/mol, which is overestimated at the Hartree−Fock (HF) level (17.6 kcal/mol) and underestimated in DFT calculations with commonly used functionals (2.9/4.1/6.0 kcal/mol for BLYP/B3LYP/BHLYP).[19−21] Another critical issue is the relative energy of different spin states, where the DFT predictions are often very sensitive to the amount of HF exchange in the chosen functional.[22−24] To quote just one such example, a recent systematic study on the spin-state energetics of heme-related models has shown that the DFT results are highly functional-dependent but can be well correlated with CCSD(T) results for simplified mimics.[23]

The principal active species of cytochrome P450 enzymes is generally accepted to be a high-valence oxoiron(IV)-cationic porphyrin species called Compound I (Cpd I), which has three unpaired electrons and essentially degenerate doublet and quartet states that give rise to two-state reactivity.[8−10] Many theoretical model studies and combined quantum mechanical/molecular mechanical (QM/MM) calculations[24−35] (for reviews see refs 7 and 8) have been performed on Cpd I and its reactions, mostly at the DFT level. The computed DFT and DFT/MM barriers for the hydrogen abstraction reaction between Cpd I and camphor are generally considered to be on the high side in view of the high reactivity of P450 enzymes and the elusive character of Cpd I.[7−14] Given the limited reliability of DFT functionals with regard to barriers and spin

Received: June 16, 2014
Published: July 23, 2014

   dx.doi.org/10.1021/ct500522d | J. Chem. Theory Comput. 2014, 10, 3807−3820

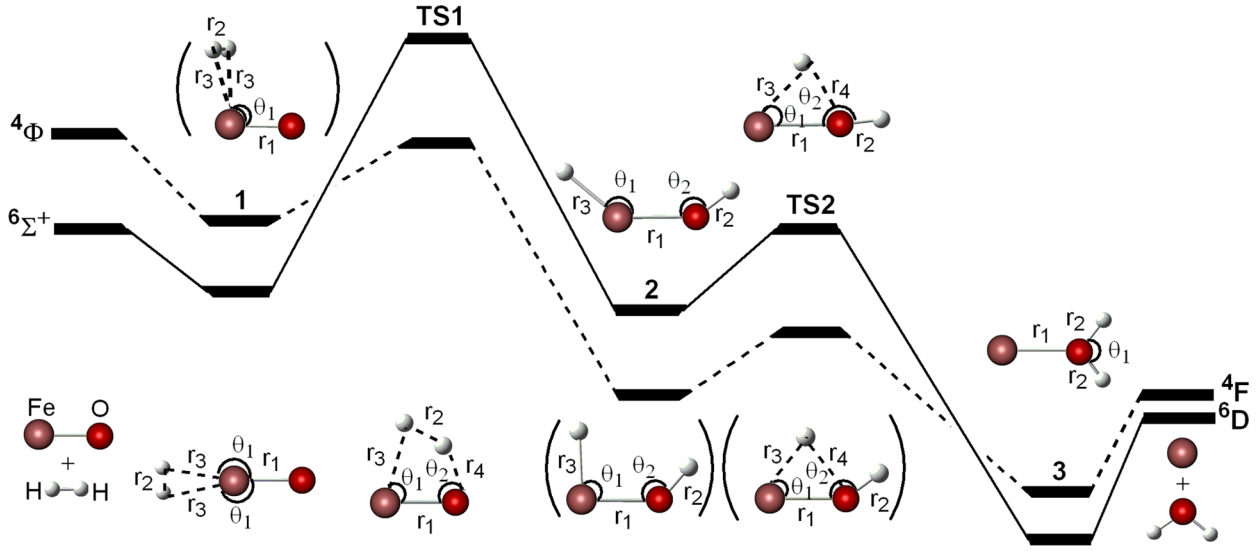

Figure 1. Qualitative two-state reactivity mechanism in the gas-phase reaction $FeO^+ + H_2 \rightarrow Fe^+ + H_2O$. The quartet-state species whose geometries differ significantly from the sextet-state species are shown in parentheses.

states (see above), it is desirable to check their accuracy by comparison with correlated ab initio studies using coupled-cluster (CC) and multireference (MR) methods. Although such large-scale calculations are demanding for realistic models of metalloenzymes and multimetallic active sites, recent advances in computing hardware and software make them possible to some extent.[7,18,34−48] It is therefore important to identify through benchmarks the best correlated ab initio approach that can be applied with confidence to such systems.

The present study compares the accuracy of various correlated ab initio methods for a related model reaction, focusing on relative spin state energies, reaction energies, and reaction barriers. We have chosen H−H bond activation by FeO^+ (see Figure 1) as the formally simplest model for hydrogen abstraction by Cpd I. This reaction has already been studied with a variety of theoretical methods, namely, DFT with the BP86, B3LYP, and FT97 functionals, CCSD(T), CASPT2D, and the diffusion quantum Monte Carlo method (DMC).[49−55] Some of these results have been summarized in an early assessment of DFT accuracy.[19] Our present work extends these previous comparisons considerably, with particular emphasis on multireference configuration interaction and related approaches. We focus on benchmarking and validation, mostly with regard to energetics, and refer the reader to the earlier studies[19,49−55] for a discussion of the mechanistic insights gained from such calculations.

■ COMPUTATIONAL METHODS

To assess the influence of the basis set on the computed properties, a series of basis sets was employed: (a) a triple-ζ basis augmented by two sets of polarization functions (TZVPP),[56,57] (17s11p6d1f)/[6s4p3d1f] for iron, (11s6p2d1f)/[5s3p2d1f] for oxygen, and (5s2p1d)/[3s2p1d] for hydrogen; (b) an atomic natural orbital (ANO) basis used in a previous CASPT2D study of this reaction,[50] (21s15p10d6f4g)/[8s7p6d4f2g] for iron, (14s9p4d3f)/[5s4p3d2f] for oxygen, and (8s4p3d)/[3s2p1d] for hydrogen; (c) a quadruple-ζ segmented contracted basis augmented by two sets of polarization functions (def2-QZVPP),[58,59] (24s18p10d3f2g)/[11s6p5d3f2g] for iron, (15s8p3d2f1g)/[7s4p3d2f1g] for oxygen, and (7s3p2d1f)/ [4s3p2d1f] for hydrogen; (d) the correlation consistent valence double-ζ basis (cc-pVDZ),[60] (20s16p8d2f)/[6s5p3d1f] for iron, (9s4p1d)/[3s2p1d] for oxygen, and (4s1p)/[2s1p] for hydrogen; (e) the correlation consistent valence triple-ζ basis (cc-pVTZ),[60] (20s16p8d2f1g)/[7s6p4d2f1g] for iron, (10s5p2d1f)/[4s3p2d1f] for oxygen, and (5s2p1d)/[3s2p1d] for hydrogen; (f) the correlation consistent valence quadruple-ζ basis (cc-pVQZ),[60] (22s18p11d3f2g1h)/[8s7p5d3f2g1h] for iron, (12s6p3d2f1g)/[5s4p3d2f1g] for oxygen, and (6s3p2d1f)/[4s3p2d1f] for hydrogen; (g) the correlation consistent weighted core−valence triple-ζ basis (cc-pwCVTZ),[60] (22s18p10d3f2g)/[9s8p6d3f2g] for iron, (12s7p3d1f)/[6s5p3d1f] for oxygen, and same as cc-pVTZ for hydrogen; (h) the correlation consistent weighted core−valence quadruple-ζ basis (cc-pwCVQZ),[60] (24s20p13d4f3g2h)/[10s9p7d4f3g2h] for iron, (15s9p5d3f1g)/[8s7p5d3f1g] for oxygen, and same as cc-pVQZ for hydrogen.

Scalar relativistic effects were investigated with the use of the second-order Douglas−Kroll−Hess Hamiltonian (DKH2)[61,62] and employing the following basis sets: (a) recontracted TZVPP (TZVPP-DKH),[56,57] (17s11p6d1f)/[10s6p3d1f] for iron, (11s6p2d1f)/[6s3p2d1f] for oxygen, and same as TZVPP for hydrogen; (b) recontracted def2-QZVPP (def2-QZVPP-DKH),[58,59] (24s18p10d3f2g)/ [14s10p5d3f2g] for iron, (15s8p3d2f1g)/[8s4p3d2f1g] for oxygen, and same as def2-QZVPP for hydrogen; (c) cc-pVQZ[60] used as is (d) cc-pwCV*n*Z-DK (n = T,Q)[60] with the same contraction scheme as the corresponding cc-pwCV*n*Z basis, but with different exponents. The results for the DKH2 Hamiltonian were always obtained with the relativistic variants of the basis sets; this will not be specified explicitly in the following. It has been established in previous work that the very flexible def2-QZVPP-DKH basis provides accurate results for scalar relativistic corrections.[59]

In our standard ab initio calculations, the core orbitals were frozen, and no virtual orbitals were neglected. The effects of core−valence electron correlation (involving 3s and 3p for iron and 1s for oxygen) were examined using the weighted core−valence (CV) basis sets of the type cc-pwCV*n*Z. The inclusion

of CV corrections in the calculations will be denoted by appending the label "+CV" to the name of the method.

One major purpose of this study is to examine which correlated ab initio methods can be applied with confidence to large systems such as the active site of heme proteins. In such applications, it is currently impractical to use large basis sets (say beyond TZVPP or ANO-type basis sets). Therefore, one aspect of our study is to assess the magnitude of the error in the calculated relative energies when using medium-sized basis sets, compared with the complete basis set (CBS) limit.

The results of correlated ab initio calculations with correlation consistent basis sets, that is, cc-p(wC)V*n*Z with n = 3 and 4, were extrapolated to the CBS limit with a two-point scheme:[63] the reference energy [unrestricted HF or recanonicalized B3LYP energy in coupled cluster calculations; CASSCF energy in the other ab initio calculations] and the correlation energy were extrapolated using

$$E_{\mathrm{ref}}^{(\infty)} = E_{\mathrm{ref}}^{(n)} - A\cdot\exp(-\alpha\sqrt{n})$$

and

$$E_{\mathrm{corr}}^{(\infty)} = \frac{n^{\beta}E_{\mathrm{corr}}^{(n)} - m^{\beta}E_{\mathrm{corr}}^{(m)}}{n^{\beta} - m^{\beta}}$$

where $E^{(n)}$ and $E^{(m)}$ are the energies obtained with a basis set of $n-\zeta$ and $m-\zeta$ cardinality (here n = 3 and m = 4), respectively, and $E^{(\infty)}$ is the CBS energy. For the constants in these expressions, we adopted the optimized values from the ORCA[64] program package for the 3/4 extrapolation with cc-pV*n*Z basis sets [α = 5.46; β = 3; A = 16653.365· ($E_{\mathrm{ref}}^{(3)} - E_{\mathrm{ref}}^{(4)}$)].[65] Since DFT calculations converge to the CBS limit much faster than correlated ab initio treatments, we did not apply any basis set incompleteness correction to the DFT energies.

Geometry optimizations were carried out with several DFT functionals and the CASSCF method using the Gaussian09 program.[66] The quadratic SCF convergence procedure was applied along with the keyword "stable=opt" in the DFT calculations to ensure the stability of the Kohn−Sham solutions. Although this procedure slowed down the convergence significantly, it always resulted in the lowest-energy electronic states of the investigated open-shell molecules that sometimes tended to converge to higher-energy excited states with the regular DIIS extrapolation.

Zero-point energies (ZPE) were evaluated at the B3LYP/TZVPP[67−69] geometries unless stated otherwise. Single-point energies for other computational methods were generally also computed at the optimized B3LYP/TZVPP geometries. Single-point DFT calculations were performed with the Gaussian09 program[66] for B3LYP (hybrid, 20% HF exchange),[67−69] its long-range corrected variant CAM-B3LYP,[70] and the meta-GGA Minnesota functionals [M05 (hybrid, 26% HF exchange), M06 (hybrid, 27% HF exchange), M06L (local, 0% HF exchange), M062X (hybrid, 54% HF exchange), and M06HF (hybrid, 100% HF exchange)].[71] The ORCA program[64] was used for the other functionals, that is, gradient corrected pure functionals [BP86,[67,72] PBE,[73] BLYP,[67,68] XLYP,[74] OLYP[75]], their hybrid versions [B1P (one-parameter hybrid BP86, 25% HF exchange),[67,72,75,76] B3P (three-parameter hybrid BP86, 20% HF exchange),[69,72,75,76] PBE0 (one-parameter hybrid PBE, 25% HF exchange),[77] B1LYP (one-parameter hybrid BLYP, 25% HF exchange),[67−69] B3LYP[67−69] in conjunction with the DKH2 Hamiltonian, BHLYP (50% HF exchange),[68,78] X3LYP (three-parameter hybrid XLYP, 21.8% HF exchange),[74] and O3LYP (three-parameter hybrid OLYP, 12% HF exchange)[75]], meta-GGA functionals [TPSS, TPSSh (hybrid TPSS, 10% HF exchange), and TPSS0 (hybrid TPSS, 25% HF exchange],[79] and the double hybrid functional B2PLYP[80] that mixes BLYP incorporating 53% HF exchange and MP2 correlation with and without D3 dispersion correction.[81]

Single-point coupled cluster (CC) calculations were done at different excitation levels,[82−86] ranging (in standard notation) from CCSD via CCSD[T], CCSD(T), CCSDT, CCSDT[Q] up to CCSDT(Q). At the unrestricted CCSDT(Q) level, we could afford calculations based on single-reference UHF wave functions using TZVPP, cc-pVDZ, and cc-pVTZ basis sets. These high-order CC calculations with single, double, triple, and perturbative quadruple excitations were performed by using the MRCC code[87] through the CFOUR package,[88] with the stability of the UHF reference being analyzed automatically through the hfstability module in CFOUR. The ORCA package was employed to run the CCSD(T) calculations with larger basis sets on top of either unrestricted HF or KS (B3LYP) orbitals.

In the MR ab initio calculations, the zero-order wave function was obtained from a complete-active-space self-consistent field (CASSCF) treatment,[89] which captures the major part of static electron correlation at the full configuration interaction (CI) level in a restricted orbital space. Since all bonds change drastically during the model reaction under study, a full-valence CAS is the only chemically sensible choice of reference space. In our standard calculations, the number of (electrons, orbitals) in the active space was as follows: (2,2) for H_2, (8,6) for H_2O, (7,6) for $Fe^+(^6D)$, (7,5) for $Fe^+(^4F)$, (13,10) for FeO^+, and (15,12) for the other species shown in Figure 1. The effect of 4d shell on the excitation energy of Fe^+ was investigated with larger active spaces of (7,11) for ^6D and (7,10) for ^4F. Second-order perturbation theory calculations[90,91] of CASPT2 (RSPT2) and diagonal CASPT2 (i.e., CASPT2D or RSPT2D) type were performed on top of the CASSCF wave function using the MOLPRO program.[92] The CASPT2 implementation of MOLPRO (i.e, RSPT2) differs slightly from the original CASPT2 formalism[93] by keeping certain configuration subspaces uncontracted in order to avoid possible bottlenecks arising from the need to handle potentially large overlap matrices. These two CASPT2 formulations generally give very similar numerical results.[90,91]

All other single-point ab initio MR calculations reported in this work were done with the ORCA program.[64] They were based on CASSCF reference wave functions. The CASSCF solutions were verified to be identical to those produced by the MOLPRO program for all species considered. Since a large number of post-CASSCF methods were investigated, we briefly comment on the methodological strategy that underlies these MR calculations.

The MR module of the ORCA package (orca_mrci) is based on spin-adapted and uncontracted configuration state functions (CSFs). The orbital space is partitioned as in CASSCF into an internal space (always doubly occupied in the reference CSFs), an active space (variable occupation) and an external space (always unoccupied in the references). The reference spaces were always of the CAS type in the present work. Large CAS spaces almost invariably contain a large number of unimportant CSFs, which greatly add to the computational expense of the calculations by bringing in a huge number of excited CSFs that do not interact with the reference wave function to second

order in perturbation theory and therefore do not belong to the first-order-interacting space (FOIS).[94] The reference spaces are therefore truncated using a threshold T_{pre}. Configurations that have a weight of less than T_{pre} in the reference wave function (after summing over all linearly independent spin-couplings) are rejected from the active space. Enumeration of all possible single and double excitations at the orbital level relative to the surviving reference CSFs leads to 13 classes of excitations[95] that are further distinguished by their "degrees of freedom". A degree of freedom is a hole in the internal subspace or a particle in the external subspace.[96] This leads to zero to four degrees of freedom in MR calculations with single and double excitations.[96] The MR correlation module of ORCA can utilize the concept of individual selection[97,98] in order to truncate the enormous FOIS that results from all single and double excitations out of the reference CSFs. CSFs from the FOIS are included or rejected from the variational subspace according to their contribution to the diagonal second-order multi-reference Møller−Plesset (MRMP2) energy using a threshold T_{sel}. The sum of the MRMP2 energies of the rejected CSFs provides an estimate of the missing correlation energy due to the selection.

The remaining list of reference and strongly interacting CSFs from the FOIS is taken as a basis for either a second-order perturbational treatment (MRMP2[99]) or a (quasi) variational configuration interaction (CI) treatment with single and double excitations (MRCISD, or simply MRCI[100]). An MR Davidson correction (+Q correction) is added to the correlation energy obtained from secular equations, in order to approximately account for the effect of neglected higher excitations (i.e., disconnected quadruples).[101] The list of interacting CSFs may well be further truncated if energy differences rather than absolute correlation energies are of importance.[102] This leads to difference-dedicated CI (DDCI) approaches: DDCI2 keeps all CSFs in the FOIS with up to two degrees of freedom, and DDCI3 those with up to three degrees of freedom. Thus, the latter approach only neglects the largest class of inactive double excitations that promote two electrons from the internal to the external subspace. Such CSFs do not contribute to energy differences up to second order in perturbation theory but affect size-consistency errors. Their effect may be estimated by the corresponding MRMP2 energy contribution.[103] In this study, DDCI-type methods are identical to MRCISD since we use the full-valence CAS.

For large molecular systems, it may be important to include corrections for the size-consistency error of the wave function into the solution of the CI equations. This can be accomplished elegantly and efficiently through a shift of the diagonal energies of the CSFs[104] in the FOIS by a number of procedures, for example, the MR averaged coupled pair functional (MRACPF) approach.[105,106] MRACPF calculations are approximately size consistent as long as the reference space is size consistent. In the ORCA implementation, the shift is applied to all CSFs that do not represent excitations that occur only inside the active space. The correlation energy is redefined in each of the MRACPF iterations using the "relaxed" reference space coefficients as the energy difference between the value of the ACPF functional and the expectation value of the Hamiltonian over the reference part of the wave function. One problem that is frequently met in MRACPF calculations is of the "intruder-state" type. A downshift of the excited CSFs (especially of single excitations) may lead to CSFs with lower diagonal energies than the references, which will dominate the wave function and invalidate the entire approach. This problem is largely absent in the MR average quadratic coupled cluster (MRAQCC) method.[107] Therefore, we only report MRAQCC results in the following.

In the present work, we evaluate two further approaches. The spectroscopy-oriented CI (SORCI[95]) method may be viewed as an individually selecting approximation to the iterative DDCI3 method.[102] In SORCI, a DDCI2 calculation is followed by a DDCI3 calculation in a truncated basis of the approximate average natural orbitals (AANOs) of the DDCI2 calculation. The truncation of the one-particle space is controlled by a third threshold T_{nat}. AANOs with an occupation number larger than $2.0 - T_{nat}$ are frozen for the final DDCI3 step while AANOs with an occupation number of less than T_{nat} are rejected. This leads to substantial savings of computer time in calculations on large molecules, since the DDCI2 CSF list only grows as $O(N^2)$ and the following DDCI3 calculation remains feasible due to the strongly truncated single-particle basis. As the SORCI method is size-inconsistent, we also tested a variant called SORCP (spectroscopy-oriented coupled pair method) in which the final DDCI3 step is replaced by an ACPF-type step. The initial DDCI2 step was kept since it is quite stable even in the case of poor starting orbitals; it has only a very moderate size-inconsistency error.

We also applied the strongly contracted version of *N*-Electron Valence State Perturbation Theory (NEVPT2).[108−111] This internally contracted MR method is based on the CASSCF wave function (and hence part of the orca_casscf module). The calculation of NEVPT2 energies generally requires less time than the CASSCF iterations and inherits all settings from CASSCF in the ORCA implementation. NEVPT2 calculations are size consistent and do not suffer from any intruder state problem.

Finally, we examined the effects of the thresholds on the MRCI results. Relative energies vary up to 3 kcal/mol when tightening T_{sel} from 10^{-6} to 10^{-8} whereas there are only negligible changes when tightening T_{pre} from 10^{-4} to 10^{-6} and T_{nat} (used only for SORCI) from 10^{-5} E_h to 10^{-7} E_h. The absolute energies are well converged with $T_{sel} = 10^{-8}$ and $T_{pre} = 10^{-5}$. For example, the MRCI+Q/cc-pVQZ energy of the sextet FeO^+ is −1337.4979 E_h with $T_{sel} = 10^{-8}$ and $T_{pre} = 10^{-5}$ or 10^{-6}, which is almost identical to the CCSD(T)/cc-pVQZ energy of −1337.4983 E_h (difference: 0.26 kcal/mol). By contrast, this deviation increases to 6 kcal/mol with the looser thresholds $T_{sel} = 10^{-6}$ and $T_{sel} = 10^{-4}$. Unless stated otherwise, we present in the following the results with $T_{sel} = 10^{-8}$, $T_{pre} = 10^{-6}$, and $T_{nat} = 10^{-7}$.

In this study, improved virtual orbitals were not used in any correlated ab initio calculation. In all perturbative treatments except NEVPT2 and B2PLYP, a level shift of 0.4 E_h was applied to avoid intruder state problems.

RESULTS AND DISCUSSION

Overview. As described in the preceding section, the present computational study is quite comprehensive. For the calculation of energies, we have used six variants of coupled cluster theory, 22 density functionals of different flavors, and eight correlated multireference ab initio methods, in combination with eight extended basis sets and with extrapolation to the CBS limit in the ab initio case. Furthermore, we have evaluated DKH2, CV, and ZPE corrections to the energies (usually again at different levels) and have explored the effects of various computational options in the ab initio multireference

calculations (Davidson correction, choice of active space, thresholds, etc.). The numerical results obtained are fully documented in the Supporting Information (Tables S1−S13). In the following, we only present what we consider the most important results.

Geometries. Optimized geometries were obtained for each stationary point on the sextet and quartet potential energy surfaces (see Figure 1) at the BP86, TPSS, B3LYP, BHLYP, and full-valence CASSCF levels using the TZVPP basis. The results are collected in Tables S1 and S2 of the Supporting Information. Species ^{6}**1** and **3** (^{4}**1**, **2**, **TS1**, and ^{6}**TS2**) adopt C_{2v} (C_s) symmetry, whereas the nonplanar transition state ^{4}**TS2** has no symmetry (the left superscript denotes the multiplicity). BP86, TPSS, and B3LYP distances (angles) agree typically within 0.03 Å (3°); exceptions are the H−Fe−O angle in ^{4}**2** and the parameters defining the position of the migrating hydrogen in ^{6}**TS2** and of H_2 in ^{4}**1**. The BHLYP and CASSCF results often differ significantly from each other, as well as from the BP86 and B3LYP values; for example, the Fe−O distance and the H−Fe−O tilt angle in ^{4}**1** from BHLYP are much larger than those obtained from the other methods (by ca. 0.2 Å and 60°, respectively). The BHLYP results for the quartet species are probably not reliable, because they suffer from large spin contamination (computed S^2 values too high by 0.5−1.0) while the other functionals give essentially pure quartet states, except for $^4FeO^+$ with a deviation of ∼0.7 from the ideal S^2 value. The present BP86 and B3LYP geometries are consistent with those obtained previously.[52]

The Fe−O bond length of $^6FeO^+$ was determined experimentally as r_0 = 1.643 ± 0.001 Å in ref 112 and as r_0 = 1.641 ± 0.001 Å in ref 113, which corresponds to an equilibrium bond length of r_e = 1.638 Å.[112] The B3LYP (TZVPP: 1.633 Å; cc-pVQZ: 1.636 Å) and BP86 (TZVPP: 1.632 Å) equilibrium bond lengths agree very well with experiment.[112,113] However, BHLYP/TZVPP (1.654 Å) and especially CASSCF/TZVPP (1.698 Å) overestimate the equilibrium bond length significantly, while CCSD(T) underestimates it somewhat (TZVPP: 1.627 Å; cc-pVQZ: 1.626 Å). Inclusion of core−valence corrections shortens the CCSD(T) bond length further (cc-pVQZ: 1.615 Å).

The BP86 and B3LYP functionals are generally known to give realistic structures for transition metal compounds,[19,114−116] and it is thus not surprising that the BP86/TZVPP- and B3LYP/TZVPP-optimized geometries appear reasonable also in the present case. The B3LYP/TZVPP geometries were used for most of the single-point energy evaluations described in the following.

Energy Profiles Compared with Previous Studies. Table S3 of the Supporting Information lists the energies of all stationary points (see Figure 1) relative to the sextet entrance channel ($^6FeO^+$ + H_2) from published earlier calculations[49,50,52,54,55] and from analogous present calculations to facilitate comparisons. Quantitative agreement with earlier studies cannot be expected since the chosen basis sets and thus the geometries are not exactly identical. The present BP86 and B3LYP results are very similar to those reported by Filatov and Shaik,[52] with the exception of the BP86 relative energies of Fe^+ that are 10 kcal/mol higher in ref 52 (indicating convergence to a higher-lying state). There are occasional deviations between the present and other published B3LYP results,[49,55] which range up to 7 kcal/mol.

The previous CASPT2D/ANO calculations[50] were performed at geometries optimized with a pure density functional and a small basis set of double-ζ quality, while the current CASPT2D/ANO results refer to BP86/TZVPP geometries. The largest deviations of ca. 9 (6) kcal/mol for ^{6}**1** ($^4FeO^+$ + H_2) are mainly due to differences in the Fe−O bond length (e.g., in the quartet species smaller by 0.04 Å in the previous study). The use of Cartesian (spherical harmonics) basis functions in the previous (present) calculations accounts only for discrepancies up to 0.3 kcal/mol (according to test calculations).

All published CCSD(T) energies were evaluated at B3LYP geometries obtained with triple-ζ quality basis sets[49,55] and include ZPE corrections. To allow for direct comparisons, we have also added ZPE corrections evaluated at the B3LYP/TZVPP level to our CCSD(T) energies. ZPE values of H_2, H_2O, and FeO^+ are available in literature: H_2, 2179.3 ± 0.1 cm^{-1} (6.2 kcal/mol; exp.[117]); H_2O, 4638.31 cm^{-1} (13.3 kcal/mol; accurate rovibrational ab initio result[118]); and FeO^+, 419 ± 2 cm^{-1} (1.2 kcal/mol; exp.[119]). The corresponding B3LYP/TZVPP values are 2209.6 cm^{-1} (6.3 kcal/mol), 4677.2 cm^{-1} (13.4 kcal/mol), and 422.0 cm^{-1} (1.2 kcal/mol), respectively. Evidently, they agree perfectly with the available experimental and ab initio data.

Our ZPE-corrected CCSD(T)/TZVPP relative energies for a UHF reference function deviate from previously published data[49] by 6 kcal/mol for Fe^+ and ^{4}**3** but agree reasonably well for the other species (Supporting Information Table S3). The best previous CCSD(T) results[55] were obtained using large correlation consistent basis sets, a restricted open-shell KS(B3LYP) reference, and CV, DKH2, and ZPE energy corrections. They agree with corresponding CCSD(T) results from the present study typically to within 2 kcal/mol for all species. The previous work[55] also reported coupled cluster results obtained with UKS(B3LYP) and Brueckner orbitals and with explicitly correlated treatments.

In an overall assessment, when taking into account differences with regard to basis sets and geometries, the present results are consistent with the previously published relative energies.

Influence of the Chosen Computational Options on Relative Energies. CASPT2/TZVPP and CASPT2D/TZVPP calculations at BP86/TZVPP geometries yield essentially the same relative energies (Supporting Information Table S3) indicating that the neglect of off-diagonal Fock matrix elements in CASPT2D is a good approximation in our case. When improving the basis from TZVPP to ANO, the change in the CASPT2D relative energies is normally about 2 kcal/mol, but it may reach 7 kcal/mol (^{6}**2**) or even 8.4 kcal/mol (excitation energy of Fe^+). The typical change in relative energies when going from TZVPP to cc-pV*n*Z (*n* = 3 or 4) is 3−6 kcal/mol for the majority of the species (especially in the quartet state) in the CASPT2 and MR calculations performed (Supporting Information Tables S3, S9, and S10). It is even larger for SORCI and SORCP (around 10 kcal/mol for the reaction energy and above 8 kcal/mol for the excitation energy of Fe^+). The MR relative energies with cc-pVQZ, cc-pwCVQZ and def2-QZVPP are almost identical and differ from those with their triple-ζ counterparts slightly (maximum deviations of ∼2 kcal/mol for **3** and Fe^+). The results from these computational tests document the need to go beyond the commonly used TZVPP basis set in the ab initio treatments.

By contrast, enlarging the basis from TZVPP to ANO or to cc-p(wC)V*n*Z does not affect the DFT relative energies much in general, except for ^{4}**3** and Fe^+ (Supporting Information

Tables S3 and S7). This supports the use of the TZVPP basis set in DFT calculations of large iron-containing molecules (e.g., the species in the P450 catalytic cycle). For a given functional, the single-point DFT relative energies are essentially the same when using BP86, B3LYP, and TPSS geometries (except for ^{4}**TS1**, see Supporting Information Table S3), whereas they are quite different when using the BHLYP or CASSCF geometries with larger bond lengths. Although the DFT energy of ^{4}**TS1** is strongly geometry-dependent (at BP86, B3LYP, BHLYP, and TPSS geometries), CASPT2 yields essentially the same ^{4}**TS1** energy at the BP86 and B3LYP geometries (Supporting Information Table S3).

The relativistic DKH2 corrections to the relative energies (Supporting Information Tables S4, S5, S7, S8, S10, and S11) depend only slightly on the chosen basis set or method (CC, DFT, or MR) although there are some occasional deviations. In the CBS extrapolation of the CC and MR energies, we evaluate the DKH2 correction for a given method using the def2-QZVPP basis set, which was shown to yield accurate results in previous work.[59] By contrast, the core−valence (CV) correlation corrections depend rather strongly on the choice of basis set and method (Supporting Information Tables S4, S5, S7, S8, S10, and S11). Therefore, we determine these corrections for the CBS extrapolation from calculations with the large cc-pwCVQZ basis, which was designed for this purpose. MR calculations of the CV corrections are problematic in our system, as can be seen from the results for the quartet/sextet energy difference in Fe^+: MR calculations using the standard active space give a CV correction of ∼7 kcal/mol, which vanishes almost entirely (in agreement with the CCSD(T) results) when the active space is enlarged to include the 4d shell (Supporting Information Table S12). Moreover, the computed MR relative energies generally deteriorate significantly when adding CV corrections from MR calculations with the standard active space. Both these observations indicate that the inclusion of the 4d shell in the active space is essential for the proper MR calculation of CV corrections. Since this is very costly even for our small benchmark system, we correct the MR relative energies in the following by adding the CV corrections from our CCSD(T) calculations. Test calculations confirm that the DKH2 and CV contributions are essentially additive, as expected.

In the remainder of this section, we only discuss the results obtained at optimized B3LYP/TZVPP geometries.

Energy Profiles with Single-reference Methods. We adopt coupled cluster methods for single-reference benchmarks. The CCSD(T) relative energies obtained using the UHF and UKS references agree with each other to within 3 kcal/mol (Supporting Information Tables S4 and S5) and likewise with previous CCSD(T) results.[55] However, the values for the T_1 diagnostic are much smaller with UKS than with UHF orbitals for the majority of the species (Supporting Information Table S6) as also observed previously.[55] This indicates that the large T_1 values obtained with UHF orbitals do not primarily arise from the multireference character of the species[120,121] but from not including electronic correlation effects at the orbital level (as in UKS).[55] The CFOUR program package[88] allows treating excitations higher than triples only with a UHF reference. We assume that such higher-order CC calculations with UHF and UKS orbitals would also give similar results, as in the CCSD(T) case. In the following, we only discuss the UHF-based CC results and refer the reader to the Supporting Information for the UKS-based CC results (Table S5).

Basis set extension causes non-negligible variations in the CC relative energies, which underlines the importance of extrapolating them to the CBS limit (Table 1). The effect of the perturbative triples on the reaction profile is large, especially for species on the quartet surface. Going from perturbative triples to full triples leads to changes in the relative energies of up to 2 kcal/mol [T−(T), cc-pVTZ basis]. CCSDT calculations with full triples and the cc-pVQZ basis set become prohibitively expensive for some of the stationary points considered. Whenever these calculations were affordable, the T−(T) corrections with the cc-pVTZ and cc-pVQZ basis sets agree to within 0.5 kcal/mol (Supporting Information Table S4), which supports the consistent use of T−(T)/cc-pVTZ values in the benchmarking. The corrections from the perturbative quadruple excitations (Q) on the relative energies are almost identical for the cc-pVDZ and cc-pVTZ basis sets, indicating that the (Q) contributions are already converged with the small cc-pVDZ basis set. The T−(T) and (Q) corrections computed with the cc-pVTZ basis and the DKH2 corrections from CCSD(T)/def2-QZVPP calculations were added to the CCSD(T)/CBS energies (Table 1). The resulting CCSDT(Q)+CV+DKH2+ZPE energies constitute our benchmark values for single-reference methods.

To assess the accuracy of various density functionals, we performed single-point calculations at the B3LYP/TZVPP geometries using the cc-pVQZ basis (Table 2). Relativistic DKH2 corrections were computed using the cc-pVQZ and def2-QZVPP basis sets (Supporting Information Table S7). They do not depend much on the chosen functional and basis set. The final relative DFT energies in Table 2 include DKH2 corrections from B3LYP/def2-QZVPP and ZPE corrections from B3LYP/TZVPP calculations. Table 2 also lists the mean absolute deviations (MADs) of the DFT energies from the CC benchmark values.

The pure GGA and pure meta-GGA functionals (0% HF exchange) differ appreciably from the best CC results (MAD = 6.0−9.2 kcal/mol). Their hybrid versions with 50% or more HF exchange (BHLYP, M062X, and M06HF) fail badly (MAD > 16 kcal/mol). Compared with their pure analogs, the one-parameter hybrid functionals with 25% HF exchange (B1P, PBE0, B1LYP) show only little or no improvement, whereas the three-parameter hybrid functionals with 22% or less HF exchange (B3P, B3LYP, X3LYP, O3LYP) yield MAD values that are reduced by at least 2 kcal/mol. B3LYP (20% HF) performs best in reproducing the single-reference CC benchmark data (MAD = 3.7 kcal/mol). Its long-range corrected variant CAM-B3LYP is less accurate (MAD = 6.0 kcal/mol). Alternatives to B3LYP in terms of MAD are the hybrid meta-GGA functional M06 (27% HF; MAD = 4.0 kcal/mol) and TPSSh (10% HF; MAD = 4.2 kcal/mol), while TPSS0 performs less well (25% HF; MAD = 6.0 kcal/mol). The double-hybrid B2PLYP functional that incorporates MP2 correlation and 53% HF exchange is of similar accuracy as the latter (MAD = 6.0 kcal/mol). Dispersion corrections are calculated to be small (<0.5 kcal/mol), as expected for a tetra-atomic system, and their inclusion does not improve the B2PLYP results much (Table 2).

Energy Profiles with Multireference Methods. Table 3 lists the relative energies obtained from selected ab initio methods at the optimized B3LYP/TZVPP geometries. In test calculations with the MRCI+Q, MRAQCC, and NEVPT2

Table 1. Sextet and Quartet CC Energy Profiles (kcal/mol) Relative to the $^6FeO^+ + H_2$ Reactants and Individual Corrections Calculated at B3LYP/TZVPP Geometries

method	basis set	$^6FeO^+ + H_2$	$^4FeO^+ + H_2$	^{6}1	^{4}1	^{6}TS1	^{4}TS1	^{6}2	^{4}2	^{6}TS2	^{4}TS2	^{6}3	^{4}3	$Fe^+ (^6D) + H_2O^a$	$Fe^+ (^4F) + H_2O$	$\Delta_1{}^b$	$\Delta_2{}^c$
CCSD(T)	cc-pwCVTZ	0.0	10.9	−13.8	−4.8	12.5	3	−34.4	−34.1	−8.9	−29.0	−77.7	−74.5	−42.6	−38.6	4.0	35.1
CCSD(T)	cc-pwCVQZ	0.0	10.5	−14.2	−6.1	12.1	1.8	−35.5	−36.1	−10.5	−31.0	−78.7	−76.4	−44.2	−41.8	2.4	34.5
CCSD(T)	CBS	0.0	10.5	−14.6	−6.8	12.0	1.1	−36.1	−37.4	−11.5	−32.3	−79.3	−77.7	−45.0	−43.7	1.3	34.3
+CV (CCSD(T))	cc-pwCVQZ	0.0	1.3	−0.2	0.9	0.8	0.6	0.7	−0.1	0.4	0.1	0.5	1.5	0.6	−0.6	−1.2	0.1
+DKH2 (CCSD(T))	def2-QZVPP	0.0	1.2	−0.6	0.7	−0.3	0.4	−2.8	−0.1	0.5	1.9	0.0	4.2	0.1	7.4	7.3	0.1
+T−(T)	cc-pVTZ	0.0	−1.5	−0.4	−1.9	−1.2	−1.8	1.0	−0.3	0.5	−0.1	1.9	1.8	1.9	2.0	0.1	0.0
+(Q)	cc-pVTZ	0.0	2.2	0.3	−1.0	0.3	0.5	2.9	2.4	3.3	2.7	4.4	4.1	4.2	4.2	0.0	−0.2
+ZPE (B3LYP)	TZVPP	0.0	−0.2	2.2	3.3	0.7	1.7	3.4	3.5	1.3	2.9	7.2	7.5	5.8	5.8	0.0	−1.4
CCSDT(Q) +CV+DKH2+ZPE	CBS	0.0	13.5	−13.3	−4.8	12.3	2.5	−30.9	−32.0	−5.5	−24.8	−65.3	−58.6	−32.4	−24.9	7.5	32.9

[a]Experimental: −34.9 ± 0.5 kcal/mol (refs 122 and 123). [b]Excitation energy of Fe^+ [$\Delta_1 = E(^4F) - E(^6D)$]. Experimental: 5.8 kcal/mol (refs 49 and 124) [c]Dissociation energy of 3 [$\Delta_2 = E(Fe^+) + E(H_2O) - E(Fe{-}OH_2^+)$]. Experimental value at 0 K: 30.6 ± 1.5 kcal/mol (ref 125)

methods, CBS extrapolations using the cc-pV*n*Z and the computationally much more demanding cc-pwCV*n*Z (n = 3 and 4) basis sets gave CBS energies that agree to within 1 kcal/mol (Supporting Information Table S11). Therefore, we used the less expensive cc-pV*n*Z basis sets throughout to determine the extrapolated CBS energies of all methods included in Table 3. These CBS relative energies were corrected by including DKH2 contributions from MRCI+Q/def2-QZVPP, ZPE contributions from B3LYP/TZVPP, and CV contributions from CCSD(T)/cc-pwCVQZ calculations. Table 3 contains these final relative energies as well as the corresponding MAD values with respect to the best single-reference CC benchmark data and to the MRCI+Q results (traditionally regarded as a suitable multireference benchmark).

Comparison between the CASSCF and post-CASSCF results shows that the incorporation of dynamical correlation has a major effect on the computed energy profiles. CASSCF relative energies show considerable deviations both from the CC and MRCI+Q reference data (MAD = 8.6 and 9.2 kcal/mol, respectively).

The a posteriori Davidson correction (+Q) to the energies attempts to account for the size-consistency error of MRCI and SORCI. Its effect on the relative energies is less than 2 kcal/mol for the majority of the species, but can become as large as 4 kcal/mol for ^{6}**3** and 10 (8) kcal/mol for sextet (quartet) Fe^+ (Supporting Information Table S11). The MRCI+Q and SORCI+Q reaction profiles agree reasonably well with those obtained from the approximately size-consistent MRAQCC method, as well as CASPT2 (except for sextet **2** and Fe^+). The reaction profiles of the other post-CASSCF methods (MRMP2, NEVPT2, and SORCP) deviate from the MRCI+Q profile more strongly.

The mean absolute deviations of the ab initio results with respect to the best CC benchmark values are given in the last column of Table 3. The smallest MAD value is found for SORCI+Q (1.9 kcal/mol) followed by MRAQCC (3.9 kcal/mol), MRCI+Q (4.6 kcal/mol), NEVPT2 (5.2 kcal/mol), SORCP (5.7 kcal/mol), CASPT2 (6.2 kcal/mol), CASSCF (8.6 kcal/mol), and MRMP2 (8.9 kcal/mol). The SORCI+Q relative energies lie mostly in between the MRCI+Q and the best CC energies and thus give small deviations in both comparisons.

Comparison of Computed Energies with Experiments. The large deviations among the energy profiles of the investigated computational methods call for comparisons with experiment. Unfortunately, experimental data are not available for the complete reaction profile. The following discussion of the accuracy of the methods will thus be restricted to specific comparisons with the available data.[49,122−127]

TS1 Barrier. Experiments[126,127] suggest a two-state reactivity pattern (Figure 1), involving one spin-allowed reaction (sextet path) with a barrier of ∼14 kcal/mol and another inefficient spin-forbidden reaction without any significant barrier (quartet path; approximately one of every 600 collisions of FeO^+ with H_2 is successful). The negative dependence of the reaction cross section on the relative collision energy suggests that the rate-limiting transition state ^{4}TS1 lies slightly lower in energy than the separated reactants.[55,126,127] Our single-reference benchmark method CCSDT(Q) gives TS1 barriers of 12.3 kcal/mol (sextet) and 2.5 kcal/mol (quartet), which are in a reasonable range. We note in this context that the use of UKS(B3LYP) instead of UHF orbitals lowers the TS1 barriers at the CCSD(T)/CBS

dx.doi.org/10.1021/ct500522d | J. Chem. Theory Comput. 2014, 10, 3807−3820

Table 2. Sextet and Quartet DFT/cc-pVQZ Energy Profiles (kcal/mol) Relative to the $^6FeO^+ + H_2$ Reactants Calculated at the B3LYP/TZVPP Geometries with DKH2 (B3LYP/def2-QZVPP) and ZPE (B3LYP/TZVPP) Corrections

functional	$^6FeO^+ + H_2$	$^4FeO^+ + H_2$	^{6}1	^{4}1	^{6}TS1	^{4}TS1	^{6}2	^{4}2	^{6}TS2	^{4}TS2	^{6}3	^{4}3	$Fe^+ (^6D) + H_2O$[a]	$Fe^+ (^4F) + H_2O$	Δ_1[b]	Δ_2[c]	MAD
Benchmark																	
CCSDT(Q) +CV+DKH2/CBS	0.0	13.5	−13.3	−4.8	12.3	2.5	−30.9	−32.0	−5.5	−24.8	−65.3	−58.6	−32.4	−24.9	7.5	32.9	0.0
GGA																	
BP86	0.0	14.7	−14.1	−13.0	8.4	−6.3	−30.8	−38.2	−4.9	−26.6	−46.6	−52.8	−11.4	−9.3	2.1	35.2	7.1
PBE	0.0	15.3	−14.7	−14.0	6.9	−7.6	−31.8	−39.2	−6.4	−27.9	−47.5	−53.7	−11.6	−9.3	2.3	35.9	7.6
BLYP	0.0	12.2	−12.8	−12.5	11.7	−3.7	−27.9	−36.7	−1.7	−24.0	−43.2	−52.7	−8.5	−9.7	−1.2	34.7	7.4
XLYP	0.0	11.3	−12.9	−12.8	12.0	−3.6	−27.8	−36.7	−1.6	−24.0	−43.4	−53.3	−8.3	−10.2	−1.9	35.1	7.3
OLYP	0.0	18.8	−9.0	−2.3	14.0	5.3	−24.7	−27.9	3.6	−17.4	−39.3	−47.3	−7.6	−11.3	−3.7	31.7	9.2
General Hybrid[d]																	
B1P (25% HF)	0.0	6.6	−14.0	−3.3	6.8	−0.1	−40.1	−40.3	−16.7	−33.4	−74.7	−72.6	−41.0	−32.7	8.3	33.7	7.3
B3P (20% HF)	0.0	9.4	−14.0	−5.1	7.3	−1.0	−38.2	−40.0	−13.9	−32.1	−69.2	−69.4	−35.1	−28.7	6.4	34.1	5.1
PBE0 (25% HF)	0.0	7.2	−14.1	−3.6	5.9	−0.7	−40.7	−40.7	−17.5	−34.0	−75.4	−73.0	−41.6	−32.9	8.7	33.8	7.6
B1LYP (25% HF)	0.0	3.9	−12.4	−3.1	9.8	2.5	−35.4	−38.4	−13.9	−32.4	−70.9	−77.3	−37.5	−39.8	−2.3	33.4	6.6
B3LYP (20% HF)	0.0	8.1	−13.1	−4.6	9.9	1.3	−36.0	−38.6	−11.3	−29.7	−66.5	−69.1	−32.9	−28.8	4.1	33.6	3.7
CAM-B3LYP	0.0	5.2	−14.7	2.1	7.6	4.8	−40.3	−36.2	−16.4	−34.0	−65.3	−62.6	−38.6	−35.8	2.8	26.7	6.0
BHLYP (50% HF)	0.0	−8.6	−17.1	−3.4	6.3	1.3	−47.3	−43.2	−27.3	−38.6	−95.2	−87.7	−62.0	−50.3	11.7	33.2	16.3
X3LYP (21.8% HF)	0.0	7.3	−13.6	−4.8	8.8	0.8	−37.4	−39.7	−13.1	−31.2	−69.0	−71.1	−34.7	−30.1	4.6	34.3	4.9
O3LYP (12% HF)	0.0	17.5	−13.5	−5.7	6.3	−1.2	−35.8	−38.1	−9.5	−30.0	−58.3	−63.4	−22.6	−21.3	1.3	35.7	4.6
Meta GGA																	
TPSS	0.0	10.8	−13.6	−13.5	10.3	−5.6	−28.8	−36.5	−2.4	−24.6	−44.2	−53.0	−8.8	−10.9	−2.1	35.4	7.4
M06L	0.0	14.2	−14.9	−5.8	6.1	0.4	−38.5	−35.9	−4.5	−24.5	−49.8	−53.5	−12.0	−12.5	−0.5	37.8	6.0
Hybrid Meta-GGA[d]																	
TPSSh (10% HF)	0.0	8.8	−13.5	−9.1	9.6	−2.6	−32.5	−37.1	−7.0	−27.1	−55.7	−61.0	−21.3	−20.5	0.8	34.4	4.2
TPSS0 (25% HF)	0.0	2.9	−13.4	−3.6	8.4	0.5	−38.1	−38.9	−14.9	−31.5	−71.8	−72.0	−38.3	−33.5	4.8	33.5	6.3
M05 (26% HF)	0.0	16.1	−10.5	6.0	10.1	11.3	−35.0	−31.0	−3.0	−24.3	−51.1	−62.8	−19.4	−20.0	−0.6	31.7	5.5
M06 (27% HF)	0.0	13.5	−13.1	2.8	8.2	6.3	−39.6	−35.9	−8.3	−28.4	−60.7	−63.0	−28.3	−21.2	7.1	32.4	4.0
M062X (54% HF)	0.0	−5.0	−15.4	−3.5	1.0	−1.0	−51.6	−46.6	−31.4	−45.0	−96.0	−91.1	−57.1	−50.7	6.4	38.9	17.8
M06HF (100% HF)	0.0	−35.2	−15.0	−3.1	−20.0	−3.9	−68.1	−71.4	−66.0	−76.6	−139.0	−132.9	−97.0	−80.9	16.1	42.0	42.2
Double Hybrid[d]																	
B2PLYP (53% HF)	0.0	18.0	0.3	11.3	20.7	14.3	−29.3	−29.7	−4.0	−22.0	−63.9	−67.8	−30.4	−27.8	2.6	33.5	6.0
B2PLYP-D3	0.0	18.0	0.1	11.0	20.5	14.2	−29.7	−30.2	−4.5	−22.4	−65.1	−68.8	−30.4	−27.8	2.6	34.7	5.8

[a]Experimental: −34.9 ± 0.5 kcal/mol (refs 122 and 123). [b]Excitation energy of Fe^+ [$\Delta_1 = E(^4F) - E(^6D)$]. Experimental: 5.8 kcal/mol (refs 49 and 124) [c]Dissociation energy of 3 [$\Delta_2 = E(Fe^+) + E(H_2O) - E(Fe{-}OH_2^+)$]. Experimental value at 0 K: 30.6 ± 1.5 kcal/mol (ref 125) [d]HF exchange ratio in the functionals is given in parentheses.

dx.doi.org/10.1021/ct500522d | J. Chem. Theory Comput. 2014, 10, 3807−3820

Table 3. Sextet and Quartet Ab Initio Energy Profiles (kcal/mol) Relative to the $^6FeO^+ + H_2$ Reactants with CBS Extrapolation of cc-pV*n*Z (n = 3 and 4) Energies Calculated at the B3LYP/TZVPP geometries, with DKH2 (MRCI+Q/def2-QZVPP), ZPE (B3LYP/TZVPP), and CV (CCSD(T)/cc-pwCVQZ) Corrections

method	$^6FeO^+ + H_2$	$^4FeO^+ + H_2$	^{6}1	^{4}1	^{6}TS1	^{4}TS1	^{6}2	^{4}2	^{6}TS2	^{4}TS2	^{6}3	^{4}3	$Fe^+(^6D) + H_2O^a$	$Fe^+(^4F) + H_2O$	Δ_1^b	Δ_2^c	MAD[d]	MAD[e]
MRCI+Q	0.0	13.6	−10.5	2.7	17.9	9.2	−22.0	−26.9	3.3	−18.6	−64.1	−55.1	−34.7	−23.6	11.1	29.4	0.0	4.6
MRAQCC	0.0	13.6	−11.8	1.6	16.9	8.6	−23.4	−27.7	2.5	−19.2	−64.6	−59.2	−32.8	−20.6	13.2	31.8	1.3	3.9
SORCI+Q	0.0	13.2	−11.7	−2.5	12.4	3.5	−27.2	−32.7	0.2	−24.2	−63.7	−55.2	−33.8	−22.4	11.4	29.9	3.1	1.9
SORCP	0.0	12.3	−12.5	−8.6	4.7	0.0	−31.7	−41.7	−3.6	−36.2	−58.6	−61.3	−21.4	−11.5	9.9	37.2	9.5	5.7
CASPT2	0.0	16.1	−12.7	0.1	19.6	7.8	−14.9	−26.1	8.0	−17.7	−61.1	−55.0	−24.9	−23.0	1.9	36.2	2.9	6.2
MRMP2	0.0	19.6	−11.0	5.5	19.1	7.7	−11.6	−25.0	9.9	−16.3	−54.4	−41.6	−28.0	−27.6	0.4	26.4	5.2	8.9
NEVPT2	0.0	12.1	−11.3	−6.9	13.6	−4.1	−15.7	−36.8	2.6	−27.8	−63.0	−49.7	−30.6	−35.3	−4.7	32.4	6.0	5.2
CASSCF	0.0	2.8	−7.2	−3.5	13.2	11.4	−31.7	−26.0	−2.6	−22.2	−89.5	−67.3	−60.1	−14.1	46.0	29.4	9.2	8.6
Single-Reference Benchmark																		
CCSDT(Q) +CV+DKH2/CBS	0.0	13.5	−13.3	−4.8	12.3	2.5	−30.9	−32.0	−5.5	−24.8	−65.3	−58.6	−32.4	−24.9	7.5	32.9	4.6	0.0

[a]Experimental: −34.9 ± 0.5 kcal/mol (refs 122 and 123). [b]Excitation energy of Fe^+ [$\Delta_1 = E(^4F) - E(^6D)$]. Experimental: 5.8 kcal/mol (refs 49 and 124) [c]Dissociation energy of 3 [$\Delta_2 = E(Fe^+) + E(H_2O) - E(Fe{-}OH_2^+)$]. Experimental value at 0 K: 30.6 ± 1.5 kcal/mol (ref 125) [d]Relative to MRCI+Q values. [e]Relative to CC benchmark values.

level by 2.9 kcal/mol (Supporting Information Table S5), which would result in a slightly negative benchmark energy of ^{4}TS1 (−0.4 kcal/mol) that should be regarded as our best value. The normally reliable MRCI+Q approach overestimates the TS1 barriers on both surfaces, and the same applies to MRAQCC, CASPT2, MRMP2, and CASSCF (Table 3; ^{4}TS1 energies of 8−11 kcal/mol). SORCP underestimates the sextet barrier and correctly predicts a barrierless reaction for the quartet. SORCI+Q (12.4 vs 3.5 kcal/mol) and NEVPT2 (13.6 vs −4.1 kcal/mol) are the only post-CASSCF methods that describe the initial reaction step on both surfaces reasonably. At the DFT level, the functionals BLYP, XLYP, B1LYP, B3LYP, X3LYP, TPSS, TPSSh, and TPSS0 yield TS1 energies of 8−12 kcal/mol on the sextet surface and between −4 and 3 kcal/mol on the quartet surface, which is satisfactory. The M05, M062X, M06HF, and B2PLYP functionals give unrealistic TS1 energies (Table 2).

Overall Reaction Energy. The experimental reaction energy Δ_0 for the activation of molecular hydrogen by the reaction $FeO^+ + H_2 \rightarrow Fe^+ + H_2O$ is −34.9 ± 0.5 kcal/mol at 0 K.[122,123] This value is derived from the dissociation energy D_0 of FeO^+ at 0 K (3.52 ± 0.02 eV)[122] and standard thermochemical data at 0 K for $O(^3P)$, H_2, and H_2O.[123] Table 4 lists the errors in Δ_0 with respect to the experimental value. B3P, X3LYP, and MRCI+Q reproduce Δ_0 within the experimental uncertainty of 0.5 kcal/mol. The CCSDT(Q), B1LYP, B3LYP, MRAQCC, and SORCI+Q results deviate from experiment by less than 3 kcal/mol and are thus still reasonable. The errors for CAM-B3LYP, TPSS0, and NEVPT2 range between 3 and 5 kcal/mol. All GGAs, meta-GGAs (TPSS, M06L), and the hybrid variants with more than 50% HF exchange (BHLYP, M062X, M06HF) show huge deviations of more than 20 kcal/mol. The CASSCF, CASPT2, MRMP2, and SORCP results for Δ_0 deviate from experiment by 7−25 kcal/mol and are thus also not acceptable. The Davidson correction (10 kcal/mol) to the MRCI and SORCI energies significantly improves the computed reaction energy and brings it close to the experimental value (Table 4).

Excitation Energy of Fe^+. Experimentally, the lowest ^{4}F quartet state of Fe^+ lies 5.8 kcal/mol above the ^{6}D sextet ground state (difference between the J-weighted averages of the spin−orbit levels).[49,124] This excitation energy is difficult to reproduce to high accuracy theoretically. The HF method fails badly, and DFT approaches are problematic because of their well-known preference for d^n over $d^{n-1}s^1$ configurations.[19,49,128,129] The opposite bias is found for HF-based approaches, which strongly favor the $d^{n-1}s^1$ configuration. For example, at the CASSCF level with the TZVPP basis set, the $^4F(d^7)$ state is calculated at 40 kcal/mol, corresponding to an error as large as 35 kcal/mol. In state-averaged CASSCF calculations, the $^4F(d^7)$ state appears as the 36th root in the quartet multiplicity block with all lower roots representing states that belong to the d^6s^1 configuration. It is obviously a grand challenge to compensate for this enormous bias of the reference functions in the subsequent post-CASSCF treatment.

The bias of the DFT approaches is reflected in published DFT results: for example, previous B3LYP, BP86, and FT97 calculations with triple-ζ basis sets [6-311++G(3df,p), TZ2P, and modified TZVP] yield values between −2 and −6 kcal/mol (see Δ_1 in Supporting Information Table S3),[41,44] that is, they give a quartet ground state. We obtain similar results in the present DFT calculations employing a variety of functionals and large basis sets [TZVPP, ANO, cc-p(wC)V*n*Z (n = 3, 4),

Table 4. Errors in the Overall Reaction Energy (Δ_0), Excitation Energy of Fe^+ (Δ_1), and Dissociation Energy of 3 (Δ_2) Compared to Experiment (in kcal/mol)

method	Δ_0[a]	Δ_1[b]	Δ_2[c]
CCSDT(Q)	2.5	1.7	2.3
	GGA		
BP86	23.5	−3.7	4.6
PBE	23.3	−3.5	5.3
BLYP	26.4	−7.0	4.1
XLYP	26.6	−7.7	4.5
OLYP	27.3	−9.5	1.1
	General Hybrid		
B1P	−6.1	2.5	3.1
B3P	*−0.2*	0.6	3.5
PBE0	−6.7	2.9	3.2
B1LYP	−2.6	−8.1	2.8
B3LYP	2.0	*−1.7*	3.0
CAM-B3LYP	−3.7	−3.0	−3.9
BHLYP	−27.1	5.9	2.6
X3LYP	0.2	*−1.2*	3.7
O3LYP	12.3	−4.5	5.1
	Meta GGA		
TPSS	26.1	−7.9	4.8
M06L	22.9	−6.3	7.2
	Hybrid Meta-GGA		
TPSSh	13.6	−5.0	3.8
TPSS0	*−3.4*	*−1.0*	2.9
M05	15.5	−6.4	1.1
M06	6.6	1.3	1.8
M062X	−22.2	0.6	8.3
M06HF	−62.1	10.3	11.4
	Double Hybrid		
B2PLYP	4.5	−3.2	2.9
B2PLYP-D3	4.5	−3.2	4.1
	Ab Initio		
MRCI+Q	0.2	5.3	*-1.2*
MRAQCC	2.1	7.4	1.2
SORCI+Q	1.1	5.6	*−0.7*
SORCP	13.5	4.1	6.6
CASPT2	10.0	−3.9	5.6
MRMP2	6.9	−5.4	−4.2
NEVPT2	4.3	−10.5	1.8
CASSCF	−25.2	40.2	−1.2

[a]Experimental reference for $\Delta_0 = E(Fe^+) + E(H_2O) - E(FeO^+) - E(H_2)$: −34.9 ± 0.5 kcal/mol (refs 122 and 123). [b]Experimental reference for $\Delta_1 = E(^4F) - E(^6D)$: 5.8 kcal/mol (refs 49 and 124). [c]Experimental reference at 0 K for $\Delta_2 = E(Fe^+) + E(H_2O) - E(Fe-OH_2^+)$: 30.6 ± 1.5 kcal/mol (ref 125).

and def2-QZVPP]. However, compared with the quartet state $^4F(d^7)$, the sextet state ^6D (d^6s^1) is strongly stabilized by scalar relativistic effects that arise from the occupancy of the 4s orbital and typically amount to 7−8 kcal/mol at the DFT-DKH2 level. After incorporating this relativistic correction, Δ_1 is well reproduced (within 2 kcal/mol) by B3P, B3LYP, X3LYP, TPSS0, M06, and M062X (Table 4).

The published CCSD(T)/TZVP value of 5.4 kcal/mol[49] matches experiment almost perfectly; however, basis set extension spoils this seemingly good agreement since CCSD(T)/TZVPP yields 12.6 kcal/mol (Supporting Information Table S4). When using the correlation consistent basis sets (cc-pV*n*Z), the splitting is reduced gradually when moving to larger basis sets (Supporting Information Tables S4 and S5). Extrapolation of the computed CCSD(T) energies to CBS limit yields a splitting of ca. 1.5 kcal/mol both for UHF and UKS references. The effects of higher excitations [up to CCSDT(Q)] and the CV correlation corrections are quite small, but the relativistic correction is large also at the CC level (7 kcal/mol). Incorporating all these corrections leads to a final coupled cluster value of 7.5 kcal/mol for the Δ_1 splitting, which is too large by 1.7 kcal/mol.

In post-CASSCF calculations, basis set extension from TZVPP to QZVP ([11s6p5d3f1g])[130] or ANO reduces the Δ_1 splitting by 7−8 kcal/mol (Supporting Information Table S3). This confirms that very large basis sets are required in high-level correlated ab initio methods in order to correctly reproduce the excitation energy of Fe^+. This problem is much more acute for low-valent metal ions such as Fe^+ than for the higher-valent ions Fe^{2+} − Fe^{4+} that dominate the (bio)inorganic chemistry of iron.[49,128,131] The underlying reason is that the $d^{n-1}s^1$ configurations move to progressively higher energies in higher oxidation states of the metal. This is in turn caused by the preferential stabilization of the *n*d-orbitals relative to the (*n* + 1)s orbital with increasing effective nuclear charge that is less well shielded by the remaining d-electrons compared to the remaining s-electrons.

The Δ_1 splittings calculated from post-CASSCF methods show a somewhat less pronounced dependence on basis set size for correlation consistent basis sets cc-pV*n*Z (less than −2 kcal/mol for $n = 3 \rightarrow 4$). Extrapolation to the CBS limit yields Δ_1 values between 4 and 7 kcal/mol for standard MRCI+Q, MRAQCC, SORCI+Q, and SORCP (Supporting Information Table S11). The CV correlation correction obtained with these methods is around 7 kcal/mol when using our standard active space, but practically vanishes when the active space is enlarged to include 4d valence orbitals; note that the CV correction is also negligible at the CCSD(T) level. Consistent with previous MRCI+Q calculations,[129] the scalar relativistic correction is again computed to be large (∼7 kcal/mol) for these methods at the DKH2 level, and it does not change notably upon inclusion of 4d orbitals in the active space. After taking the relativistic DKH2 correction and the proper CV correlation correction (large active space) into account (Table 3), these MR methods overestimate the Δ_1 splitting by ∼5 kcal/mol (Table 4). By contrast, the second-order perturbation methods CASPT2, MRMP2, and NEVPT2 underestimate the Δ_1 splitting by 4−11 kcal/mol when the DKH2 and CV corrections are included (Table 4).

The previous MRCI+Q[129] and present MRAQCC spin−orbit coupling (SOC) calculations using a spin−orbit mean-field operator reproduce the experimental[124] spin−orbit splitting of both the ^6D and ^4F states of Fe^+ to within 30 cm^{-1} but improve the Δ_1 gap by only 0.5 kcal/mol. Therefore, SOC effects have only a very minor influence on the Δ_1 splitting.

Dissociation Energy of $Fe-OH_2^+$. The experimental dissociation energy (Δ_2) of $Fe-OH_2^+$ (**3**) is 30.6 ± 1.5 kcal/mol at 0 K.[125] Two other less accurate experimental values have been reported without specifying the temperature (28.8 ± 3.0 and 32.8 ± 4.0 kcal/mol).[49] Both the ZPE correction (−1.4 kcal/mol at the B3LYP/TZVPP level) and the CV correlation correction (∼2 kcal/mol) for the dissociation energy are of the order of the experimental uncertainty. Scalar relativistic effects (DKH2) do not contribute significantly to Δ_2. The computed dissociation energy is increased by 6 kcal/mol when adding the

dx.doi.org/10.1021/ct500522d | J. Chem. Theory Comput. 2014, 10, 3807−3820

Davidson correction (+Q) to the MRCI and SORCI values, and by 5 kcal/mol when adding the perturbative (Q) contribution to the CCSDT result.

After incorporating all corrections, the DFT functionals normally reproduce Δ_2 to within ±5 kcal/mol (Table 4), except for the M06L, M062X, and M06HF functionals. The CCSDT(Q) and most MR results are accurate to 2 kcal/mol; however, CASPT2, MRMP2, and SORCP deviate from experiment by 4−7 kcal/mol. Hence, it is apparently not too difficult to predict the dissociation energy of **3** well. This can be accomplished with the majority of the methods applied presently, both of single-reference and multireference type.

Overall Assessment. CCSDT(Q) and the hybrid density functionals B3LYP, X3LYP, and TPSS0 are the only single-reference approaches that reproduce all the available experimental data reasonably well. The reaction profiles from MRCI+Q, MRAQCC, and SORCI+Q reaction profiles are similar to each other, except for the **TS1** energies. All post-CASSCF methods have errors for the Fe^+ splitting Δ_1 of more than 3 kcal/mol. SORCI+Q is the only post-CASSCF method that reproduces all experimental data apart from the Δ_1 splitting reasonably well, including the **TS1** energies. The accuracy of SORCI+Q for excitation energies has already been established in several studies of organic compounds with truncated active spaces.[132−134] The improvement of SORCI+Q over MRCI+Q is actually not surprising in the present case. Although SORCI is only an approximation to the DDCI3 approach, DDCI-type methods are equivalent to full MRCI when using a full valence active space as in this study. Here, SORCI+Q is thus an advance over MRCI+Q because it includes a natural orbital iteration step, which improves the quality of the orbitals in the internal and active spaces. Evidently, incorporation of such a natural orbital iteration step is beneficial.

The success of CCSDT(Q) in reproducing the available experimental data and the small value of the T_1 diagnostic with a UKS reference indicate that the reaction of molecular hydrogen with FeO^+ is mainly of single-reference rather than multireference character. Hence, for the species whose energies are not available experimentally, we have adopted the CCSDT(Q) results as reference data. CCSD(T) results (also with CV, DKH2, and ZPE corrections) have previously been used for this purpose for the currently studied reaction[55] and related systems.[135] The present results show that full inclusion of triples [i.e., the correction +T−(T)] and the perturbative treatment of quadruples [i.e., (Q)] leads to changes of up to 2 and 4 kcal/mol, respectively, so that the CCSDT(Q) relative energies differ slightly from their CCSD(T) counterparts.

At the DFT level, the relative energies calculated with B3LYP (20% HF exchange), M06 (27% HF exchange), and TPSSh (10% HF exchange) show the lowest deviations from the CCSDT(Q) reference data for the stationary points (MAD = 3.7, 4.0, and 4.2 kcal/mol, respectively; see Table 2). Functionals with 50% or more HF exchange fail badly (BHLYP, M062X, M06HF). Among the presently tested density functionals, B3LYP performs best, which provides an a posteriori validation of its common use in computational studies of iron chemistry.

For easy visual inspection, Figure 2 shows the sextet (top) and quartet (bottom) reaction profiles obtained from CCSDT(Q) (black), B3LYP (red), SORCI+Q (blue), and MRCI+Q (gray) including the appropriate CV (except for DFT), DKH2, and ZPE corrections (Tables 1−3) at B3LYP/TZVPP geometries. On the sextet surface, the CCSDT(Q) relative

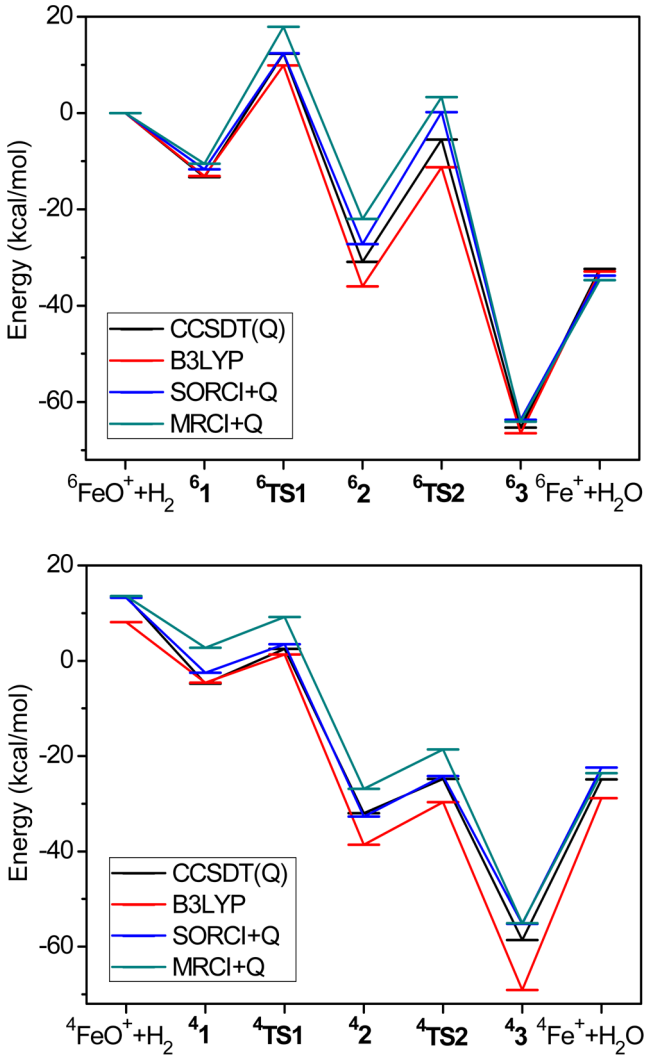

Figure 2. Sextet (top) and quartet (bottom) energy profiles from CCSDT(Q), B3LYP, SORCI+Q, and MRCI+Q calculations with CV, DKH2, and ZPE corrections at B3LYP/TZVPP geometries.

energies are slightly underestimated (overestimated) by B3LYP (SORCI+Q). On the quartet surface, B3LYP shows the same trend, while SORCI+Q closely reproduces the CCSDT(Q) data. MRCI+Q overestimates the CCSDT(Q) relative energies on both surfaces consistently.

Closer inspection of Figure 2 reveals that the calculated reaction profiles are parallel to each other in the region where hydrogen is bound, that is, between **1** and **3**, especially on the quartet surface. As discussed previously,[129,136,137] bare Fe^+ and FeO^+ are computationally difficult to handle, while higher oxidation states of iron are expected to be less problematic.[49,128,131] Iron-containing molecular species with biological relevance normally involve high-valent iron (Fe^{2+} − Fe^{4+}) with coordination numbers of four to six. Based on our present results, we expect CCSDT(Q), B3LYP, SORCI+Q, and MRCI+Q to perform well for such systems. Being computationally most efficient, B3LYP appears as the method of choice for corresponding large-scale applications. We emphasize that dispersion interactions will be much more important in these large systems than in our small benchmark case ($FeO^+ + H_2$) and that it will thus generally be advisable to include dispersion corrections in such B3LYP studies.

dx.doi.org/10.1021/ct500522d | J. Chem. Theory Comput. 2014, 10, 3807−3820

In previous ab initio multireference QM/MM work,[34] we employed DDCI2+Q calculations with a truncated active space to study some $P450_{cam}$ species, in particular two reactive intermediates (Cpd 0 and Cpd I), the transition state (TS_H) for hydrogen abstraction by Cpd I, and the resulting hydroxo intermediate (HYD). B3LYP and DDCI2+Q calculations gave similar doublet-quartet energy gaps in Cpd 0 and Cpd I, and essentially the same energy separation between TS_H and HYD. A later CASPT2/MM study on several electronic configurations of doublet and quartet Cpd I of $P450_{cam}$ also found the B3LYP results to be quite accurate.[36] In view of the present benchmark results, with fairly parallel B3LYP and MRCI+Q potential surfaces, these similarities are not surprising. We also note that in our previous work[34] the complete hydroxylation reaction path in the $P450_{cam}$ enzyme could be computed only with B3LYP but not with DDCI2+Q because this would have required prohibitively large active spaces.

CONCLUSIONS

The accuracy of CCSDT(Q), DFT, and correlated multireference multiconfiguration ab initio methods has been investigated for H_2 activation by FeO^+ in the sextet and quartet states. The reaction $FeO^+ + H_2 \rightarrow Fe^+ + H_2O$ serves as a formally simple model for hydrogen abstraction by cytochrome P450 and other large iron-containing molecules with biological relevance. The comparison of CCSDT(Q) results with the available experimental data supports the use of this coupled cluster method as reference in benchmarks. Among the density functionals, B3LYP shows the smallest deviations from the CCSDT(Q) relative energies, followed by X3LYP and TPSS0. At the multireference CI level, inclusion of the Davidson correction (+Q) for the size consistency error is beneficial, as well as the natural orbital iteration step in the SORCI approach. Among the post-CASSCF treatments, SORCI+Q reproduces the experimental data and the CCSDT(Q) relative energies best. The SORCI+Q, MRCI+Q, and MRAQCC energy profiles are generally quite parallel to each other, except for the entrance and exit channels, which contain bare FeO^+ and Fe^+ that are irrelevant in bioinorganic chemistry. Hence, it seems justified to apply any of these three MR methods to large iron-containing biomolecules. The most promising perturbational method appears to be NEVPT2, although it shows less systematic deviations from the CCSDT(Q) energies.

Core−valence correlation corrections have presently been included in all ab initio results for the sake of consistency, even though they have only a fairly minor influence on the computed relative energies. However, they may be crucial for the ordering of closely lying electronic states, as reported for some iron-bound porphyrin derivatives.[43] The scalar relativistic corrections are also small for most of the species, except for ^{4}**3** and unbound Fe^+. In the coupled cluster calculations, the effects of triple and quadruple excitations on the relative energies are moderate but non-negligible.

The present multireference calculations employed a CASSCF treatment with a full valence space, and the subsequent MRCI treatment included all single and double excitations. This approach becomes prohibitively expensive for larger systems, and there is clearly a need for approximate MR methods that only treat a rather small part of the "exploding" first-order interacting space explicitly. The DDCI and the individually selecting SORCI treatments have been designed for this purpose. One encouraging result of the present benchmark study is that the computed energy profiles from CCSDT(Q), MRCI+Q, and SORCI+Q are quite parallel to each other, indicating that simplified methods such as SORCI+Q may indeed be useful (and feasible) for ab initio studies on larger systems. We note again in this context that DDCI2+Q and B3LYP have given similar results in our previous study on an electronically demanding $P450_{cam}$ system.[34]

In practical terms, the most important outcome of our benchmark is that B3LYP indeed performs best among all tested density functionals. The B3LYP results are almost as accurate as those of the best first-principles methods for the specific reaction investigated presently, $FeO^+ + H_2 \rightarrow Fe^+ + H_2O$. Given the numerous B3LYP-based studies on heme enzymes and related systems, this is a reassuring a posteriori validation. However, it will often be still desirable in this field to check B3LYP-based predictions by correlated ab initio calculations. The present results suggest that simplified MRCI treatments such as SORCI+Q should be suitable for this purpose, since they are reasonably accurate and still affordable for studying the chemistry of large iron-containing biomolecules.

ASSOCIATED CONTENT

Supporting Information

Detailed data for the computed geometries and energy profiles. This material is available free of charge via the Internet at http://pubs.acs.org.

AUTHOR INFORMATION

Corresponding Author

*Phone: +49-208-306-2150. Fax: +49-208-306-2996. Email: thiel@mpi-muelheim.mpg.de.

Notes

The authors declare no competing financial interest.

ACKNOWLEDGMENTS

This work was supported by the Scientific and Technological Council of Turkey (TUBITAK, BIDEB 2219 grant to A.A.) and Volkswagenstiftung (grant I/80540 to W.T.).

REFERENCES

(1) *Activation and Functionalizaton of Alkanes*; Hill, C. L., Ed.; Wiley, New York, 1989.
(2) *Selective Hydrocarbon Activation*; Davies, J. A., Watson, P. L., Liebman, J. F., Greenberg, A., Eds.; VCH Publishers, New York, 1990.
(3) Ye, S.; Geng, C.-Y.; Shaik, S.; Neese, F. *Phys. Chem. Chem. Phys.* **2013**, *15*, 8017−8030.
(4) Ye, S.; Neese, F. *Proc. Natl. Acad. Sci. U.S.A.* **2011**, *108*, 1228−1233.
(5) Xue, G.; Geng, C.; Ye, S.; Fiedler, A. T.; Neese, F.; Que, L., Jr. *Inorg. Chem.* **2013**, *52*, 3976−3984.
(6) Chen, H.; Ikeda-Saito, M.; Shaik, S. *J. Am. Chem. Soc.* **2008**, *130*, 14778−14790.
(7) Shaik, S.; Cohen, S.; Wang, Y.; Chen, H.; Kumar, D.; Thiel, W. *Chem. Rev.* **2010**, *110*, 949−1017.
(8) Shaik, S.; Kumar, D.; de Visser, S. P.; Altun, A.; Thiel, W. *Chem. Rev.* **2005**, *105*, 2279−2328.
(9) Denisov, I. G.; Makris, T. M.; Sligar, S. G.; Schlichting, I. *Chem. Rev.* **2005**, *105*, 2253−2277.
(10) *Cytochrome P450: Structure, Mechanism, and Biochemistry*, 3rd ed.; de Montellano, P. R. O., Ed.; Kluwer Academic/Plenum Publishers, New York, 2004.
(11) Dunford, H. B. *Heme Peroxidases*; Wiley-VCH: New York, 1999.

(12) *Handbook of Metalloproteins*; Messerschmidt, A., Huber, R., Poulos, T. L., Wieghardt, K., Eds.; John-Wiley and Sons: New York, 2001; Vol. *1*.
(13) Price, J. C.; Barr, E. W.; Tirupati, B.; Bollinger, J. M. J.; Krebs, C. *Biochemistry* **2003**, *42*, 7497−7508.
(14) Krebs, C.; Price, J. C.; Baldwin, J.; Saleh, L.; Green, M. T.; Bollinger, J. M. *Inorg. Chem.* **2005**, *44*, 742−757.
(15) Siegbahn, P. E. M.; Blomberg, M. R. A. *Chem. Rev.* **2000**, *100*, 421−437.
(16) Delaere, D.; Nguyen, M. T. *Chem. Phys. Lett.* **2003**, *376*, 329−337.
(17) Altun, A.; Thiel, W. *J. Phys. Chem. B* **2005**, *109*, 1268−1280.
(18) Ghosh, A.; Taylor, P. R. *Curr. Opin. Chem. Biol.* **2003**, *7*, 113−124.
(19) Koch, W.; Holthausen, M. C. *A Chemist's Guide to Density Functional Theory*, 2nd ed.; Wiley-VCH, New York, 2001.
(20) Johnson, B. G.; Gonzales, C. A.; Gill, G. M. W.; Pople, J. A. *Chem. Phys. Lett.* **1994**, *221*, 100−108.
(21) Csonka, G. I.; Johnson, B. G. *Theor. Chem. Acc.* **1998**, *99*, 158−165.
(22) Reiher, M.; Salomon, O.; Hess, B. A. *Theor. Chem. Acc.* **2001**, *107*, 48−55.
(23) Radon, M. *J. Chem. Theory Comput.* **2014**, *10*, 2306−2321.
(24) Schöneboom, J. C.; Thiel, W. *J. Phys. Chem. B* **2004**, *108*, 7468−7478.
(25) Schöneboom, J. C.; Cohen, S.; Lin, H.; Shaik, S.; Thiel, W. *J. Am. Chem. Soc.* **2004**, *126*, 4017−4034.
(26) Guallar, V.; Baik, M.; Lippard, S. J.; Friesner, R. A. *Proc. Natl. Acad. Sci. U.S.A.* **2003**, *100*, 6998−7002.
(27) Guallar, V.; Friesner, R. A. *J. Am. Chem. Soc.* **2004**, *126*, 8501−8508.
(28) Altun, A.; Guallar, V.; Friesner, R. A.; Shaik, S.; Thiel, W. *J. Am. Chem. Soc.* **2006**, *128*, 3924−3925.
(29) Altun, A.; Shaik, S.; Thiel, W. *J. Comput. Chem.* **2006**, *27*, 1324−1337.
(30) Altarsha, M.; Benighaus, T.; Kumar, D.; Thiel, W. *J. Biol. Inorg. Chem.* **2010**, *15*, 361−372.
(31) Zheng, J. J.; Altun, A.; Thiel, W. *J. Comput. Chem.* **2007**, *28*, 2147−2158.
(32) Altun, A.; Shaik, S.; Thiel, W. *J. Am. Chem. Soc.* **2007**, *129*, 8978−8987.
(33) Kumar, D.; Altun, A.; Shaik, S.; Thiel, W. *Faraday Discuss.* **2011**, *148*, 373−383.
(34) Altun, A.; Kumar, D.; Neese, F.; Thiel, W. *J. Phys. Chem. A* **2008**, *112*, 12904−12910.
(35) Schöneboom, J. C.; Neese, F.; Thiel, W. *J. Am. Chem. Soc.* **2005**, *127*, 5840−5853.
(36) Chen, H.; Song, J. S.; Lai, W. Z.; Wu, W.; Shaik, S. *J. Chem. Theory Comput.* **2010**, *6*, 940−953.
(37) Claeyssens, F.; Harvey, J. N.; Manby, F. R.; Mata, R. A.; Mulholland, A. J.; Ranaghan, K. E.; Schütz, M.; Thiel, S.; Thiel, W.; Werner, H.-J. *Angew. Chem., Int. Ed.* **2006**, *45*, 6856−6859.
(38) Mata, R. A.; Werner, H.-J.; Thiel, S.; Thiel, W. *J. Chem. Phys.* **2008**, *128*, 025104.
(39) Chen, H.; Lai, W. Z.; Shaik, S. *J. Phys. Chem. B* **2011**, *115*, 1727−1742.
(40) Oláh, J.; Harvey, J. N. *J. Phys. Chem. A* **2009**, *113*, 7338−7345.
(41) Radoń, M.; Broclawik, E. *J. Chem. Theory Comput.* **2007**, *3*, 728−734.
(42) Radoń, M.; Broclawik, E.; Pierloot, K. *J. Chem. Theory Comput.* **2011**, *7*, 898−908.
(43) Vancoillie, S.; Zhao, H.; Tran, V. T.; Hendrickx, M. F. A.; Pierloot, K. *J. Chem. Theory Comput.* **2011**, *7*, 3961−3977.
(44) Choe, Y.-K.; Hashimoto, T.; Nakano, H.; Hirao, K. *Chem. Phys. Lett.* **1998**, *295*, 380−388.
(45) Choe, Y.-K.; Nakajima, T.; Hirao, K. *J. Chem. Phys.* **1999**, *111*, 3837−3845.
(46) Jensen, K. P.; Roos, B. O.; Ryde, U. *J. Inorg. Biochem.* **2005**, *99*, 45−54.
(47) Ghosh, A.; Persson, B. J.; Taylor, P. R. *J. Biol. Inorg. Chem.* **2003**, *8*, 507−511.
(48) Chalupsky, J.; Neese, F.; Solomon, E. I.; Ryde, U.; Rulisek, L. *Inorg. Chem.* **2006**, *45*, 11051−11059.
(49) Irigoras, A.; Fowler, J. E.; Ugalde, J. M. *J. Am. Chem. Soc.* **1999**, *121*, 8549−8558.
(50) Fiedler, A.; Schröder, D.; Shaik, S.; Schwarz, H. *J. Am. Chem. Soc.* **1994**, *116*, 10734−10741.
(51) Schröder, D.; Shaik, S.; Schwarz, H. *Acc. Chem. Res.* **2000**, *33*, 139−145.
(52) Filatov, M.; Shaik, S. *J. Phys. Chem. A* **1998**, *102*, 3835−3846.
(53) Danovich, D.; Shaik, S. *J. Am. Chem. Soc.* **1997**, *119*, 1773−1786.
(54) Matxain, J. M.; Mercero, J. M.; Irigoras, A.; Ugalde, J. M. *Mol. Phys.* **2004**, *102*, 2635−2637.
(55) Harvey, J. N.; Tew, D. P. *Int. J. Mass Spectrom.* **2013**, *354*−*355*, 263−270.
(56) Ahlrichs, R.; May, K. *Phys. Chem. Chem. Phys.* **2000**, *2*, 943−945.
(57) Schäfer, A.; Huber, C.; Ahlrichs, R. *J. Chem. Phys.* **1994**, *100*, 5829−5835.
(58) Weigend, F.; Ahlrichs, R. *Phys. Chem. Chem. Phys.* **2005**, *7*, 3297−3305.
(59) Pantazis, D. A.; Chen, X. Y.; Landis, C. R.; Neese, F. *J. Chem. Theory Comput.* **2008**, *4*, 908−919.
(60) (a) Dunning, T. H., Jr. *J. Chem. Phys.* **1989**, *90*, 1007−1023. (b) Balabanov, N. B.; Peterson, K. A. *J. Chem. Phys.* **2005**, *123*, 064107/1−15. (c) Peterson, K. A.; Dunning, T. H., Jr. *J. Chem. Phys.* **2002**, *117*, 10548−10560.
(61) Nakajima, T.; Hirao, K. *Chem. Rev.* **2012**, *112*, 385−402.
(62) Reiher, M. *WIREs Comput. Mol. Sci.* **2012**, *2*, 139−149.
(63) Halkier, A.; Helgaker, T.; Jorgensen, P.; Klopper, W.; Koch, H.; Olsen, J.; Wilson, A. K. *Chem. Phys. Lett.* **1998**, *286*, 243−252.
(64) (a) Neese, F. *ORCA*, Version 2.9.1; An Ab Initio, Density Functional and Semiempirical Electronic Structure Program Package; Max-Planck Institute for Bioinorganic Chemistry: Mülheim an der Ruhr, Germany, 2012. Latest version available from http://cec.mpg.de/forum (accessed July 18, 2014). (b) Neese, F. *WIREs Comput. Mol. Sci.* **2012**, *2*, 73−78.
(65) Neese, F.; Valeev, E. F. *J. Chem. Theory Comput.* **2011**, *7*, 33−43.
(66) Frisch, M. J.; Trucks, G. W.; Schlegel, H. B.; Scuseria, G. E.; Robb, M. A.; Cheeseman, J. R.; Scalmani, G.; Barone, V.; Mennucci, B.; Petersson, G. A.; Nakatsuji, H.; Caricato, M.; Li, X.; Hratchian, H. P.; Izmaylov, A. F.; Bloino, J.; Zheng, G.; Sonnenberg, J. L.; Hada, M.; Ehara, M.; Toyota, K.; Fukuda, R.; Hasegawa, J.; Ishida, M.; Nakajima, T.; Honda, Y.; Kitao, O.; Nakai, H.; Vreven, T.; Montgomery, J. A., Jr.; Peralta, J. E.; Ogliaro, F.; Bearpark, M.; Heyd, J. J.; Brothers, E.; Kudin, K. N.; Staroverov, V. N.; Kobayashi, R.; Normand, J.; Raghavachari, K.; Rendell, A.; Burant, J. C.; Iyengar, S. S.; Tomasi, J.; Cossi, M.; Rega, N.; Millam, N. J.; Klene, M.; Knox, J. E.; Cross, J. B.; Bakken, V.; Adamo, C.; Jaramillo, J.; Gomperts, R.; Stratmann, R. E.; Yazyev, O.; Austin, A. J.; Cammi, R.; Pomelli, C.; Ochterski, J. W.; Martin, R. L.; Morokuma, K.; Zakrzewski, V. G.; Voth, G. A.; Salvador, P.; Dannenberg, J. J.; Dapprich, S.; Daniels, A. D.; Farkas, Ö.; Foresman, J. B.; Ortiz, J. V.; Cioslowski, J.; Fox, D. J. *Gaussian 09*, Revision A.02; Gaussian, Inc.; Wallingford, CT, 2009.
(67) Becke, A. D. *Phys. Rev. A* **1988**, *38*, 3098−3100.
(68) Lee, C.; Yang, W.; Parr, R. G. *Phys. Rev. B* **1988**, *37*, 785−789.
(69) Becke, A. D. *J. Chem. Phys.* **1993**, *98*, 5648−5652.
(70) Yanai, T.; Tew, D.; Handy, N. *Chem. Phys. Lett.* **2004**, *393*, 51−57.
(71) (a) Zhao, Y.; Schultz, N. E.; Truhlar, D. G. *J. Chem. Phys.* **2005**, *123*, 161103/1−4. (b) Zhao, Y.; Truhlar, D. G. *J. Chem. Phys.* **2006**, *125*, 194101/1−18. (c) Zhao, Y.; Truhlar, D. G. *Theor. Chem. Acc.* **2006**, *120*, 215−241. (d) Zhao, Y.; Truhlar, D. G. *J. Phys. Chem. A* **2006**, *110*, 13126−13130.
(72) Perdew, J. P. *Phys. Rev. B* **1986**, *33*, 8822−8824.
(73) Perdew, J. P.; Burke, K.; Ernzerhof, M. *Phys. Rev. Lett.* **1996**, *77*, 3865−3868.

(74) Xu, X.; Goddard, W. A., III *Proc. Natl. Acad. Sci. U.S.A.* **2004**, *101*, 2673−2677.
(75) Handy, N. C.; Cohen, A. *J. Mol. Phys.* **2001**, *99*, 403−412.
(76) Perdew, J. P.; Chevary, J. A.; Vosko, S. H.; Jackson, K. A.; Pederson, M. R.; Singh, D. J.; Fiolhais, C. *Phys. Rev. B* **1992**, *46*, 6671−6687.
(77) Adamo, C.; Barone, V. *J. Chem. Phys.* **1999**, *110*, 6158−6169.
(78) Becke, A. D. *J. Chem. Phys.* **1993**, *98*, 1372−1377.
(79) Tao, J.; Perdew, J. P.; Staroverov, V. N.; Scuseria, G. E. *Phys. Rev. Lett.* **2003**, *91*, 146401/1−4.
(80) Goerigk, L.; Grimme, S. *J. Chem. Theory Comput.* **2011**, *7*, 291−309.
(81) Grimme, S.; Antony, J.; Ehrlich, S.; Krieg, H. *J. Chem. Phys.* **2010**, *132*, 154104−154117.
(82) Bartlett, R. J.; Watts, J. D.; Kucharski, S. A.; Noga, J. *Chem. Phys. Lett.* **1990**, *165*, 513−522.
(83) Raghavachari, K.; Pople, J. A.; Replogle, E. S.; Gordon, H. *M. J. Phys. Chem.* **1990**, *94*, 5579−5596.
(84) Bomble, Y. J.; Stanton, J. F.; Kallay, M.; Gauss, J. *J. Chem. Phys.* **2005**, *123*, 054101/1−8.
(85) Kallay, M.; Gauss, J. *J. Chem. Phys.* **2005**, *123*, 214105/1−13.
(86) Kallay, M.; Gauss, J. *J. Chem. Phys.* **2008**, *129*, 144101/1−9.
(87) (a) Kallay, M.; Rolik, Z.; Ladjanszki, I.; Szegedy, L.; Ladoczki, B.; Csontos, J.; Kornis, B. *MRCC*; A Quantum Chemical Program Suite; see: http://www.mrcc.hu (accessed July 18, 2014); (b) Rolik, Z.; Szegedy, L.; Ladjanszki, I.; Ladoczki, B.; Kallay, M. *J. Chem. Phys.* **2013**, *139*, 094105/1−17.
(88) Stanton, J. F.; Gauss, J.; Harding, M. E.; Szalay, P. G. with contributions from Auer, A. A.; Bartlett, R. J.; Benedikt, U.; Berger, C.; Bernholdt, D. E.; Bomble, Y. J.; Christiansen, O.; Heckert, M.; Heun, O.; Huber, C.; Jagau, T.-C.; Jonsson, D.; Jusélius, J.; Klein, K.; Lauderdale, W. J.; Matthews, D. A.; Metzroth, T.; O'Neill, D. P.; Price, D. R.; Prochnow, E.; Ruud, K.; Schiffmann, F.; Stopkowicz, S.; Tajti, A.; Vázquez, J.; Wang, F.; Watts, J. D. *CFOUR*, Version 1.0; A Quantum Chemical Program Package, including the integral packages *MOLECULE* (Almlöf, J.; Taylor, P. R.), *PROPS* (Taylor, P. R.), *ABACUS* (Helgaker, T.; Jensen, H. J. Aa.; Jørgensen, P.; Olsen, J.), and *ECP* routines (Mitin, A. V.; van Wüllen, C.). See: http://www.cfour.de (accessed July 18, 2014).
(89) Roos, B. O.; Taylor, P. R. *Chem. Phys.* **1980**, *48*, 157−173.
(90) Werner, H. J. *Mol. Phys.* **1996**, *89*, 645−661.
(91) Celani, P.; Werner, H. J. *J. Chem. Phys.* **1992**, *112*, 5546−5557.
(92) Werner, H.-J.; Knowles, P. J.; Lindh, R.; Manby, F. R.; Schütz, M.; Celani, P.; Korona, T.; Mitrushenkov, A.; Rauhut, G.; Adler, T. B.; Amos, R. D.; Bernhardsson, A.; Berning, A.; Cooper, D. L.; Deegan, M. J. O.; Dobbyn, A. J.; Eckert, F.; Goll, E.; Hampel, C.; Hetzer, G.; Hrenar, T.; Knizia, G.; Köppl, C.; Liu, Y.; Lloyd, A. W.; Mata, R. A.; May, A. J.; McNicholas, S. J.; Meyer, W.; Mura, M. E.; Nicklass, A.; Palmieri, P.; Pflüger, K.; Pitzer, R.; Reiher, M.; Schumann, U.; Stoll, H.; Stone, A. J.; Tarroni, R.; Thorsteinsson, T.; Wang, M.; Wolf, A. *Molpro*, Version 2008.2, A Package of Ab Initio Programs. See: http://www.molpro.net (accessed July 18, 2014).
(93) Andersson, K.; Malmqvist, P.-A.; Roos, B. O. *J. Chem. Phys.* **1992**, *96*, 1218−1226.
(94) McLean, A. D.; Liu, B. *J. Chem. Phys.* **1973**, *58*, 1066−1078.
(95) Neese, F. *J. Chem. Phys.* **2003**, *119*, 9428−9443.
(96) Miralles, J.; Castell, O.; Caballol, R.; Malrieu, J. P. *Chem. Phys. Lett.* **1993**, *172*, 33−43.
(97) Buenker, R. J.; Peyerimhoff, S. D. *Theoret. Chim. Acta* **1974**, *35*, 33−58.
(98) Huron, B.; Malrieu, J. P.; Rancurel, P. J. *Chem. Phys.* **1973**, *58*, 5745−5759.
(99) Nakano, H. *J. Chem. Phys.* **1993**, *99*, 7983−7992.
(100) Sharp, S. B.; Gellene, G. I. *J. Chem. Phys.* **2000**, *113*, 6122−6131.
(101) Hirsch, G.; Bruna, P. J.; Peyerimhoff, S. D.; Buenker, R. J. *Chem. Phys. Lett.* **1977**, *52*, 442−448.
(102) Miralles, J.; Castell, O.; Caballol, R.; Malrieu, J. P. *Chem. Phys.* **1993**, *172*, 33−43.
(103) Castell, O.; Garcia, V. M.; Bo, C.; Caballol, R. *J. Comput. Chem.* **1996**, *17*, 42−48.
(104) Szalay, P. G.; Müller, T.; Lischka, H. *Phys. Chem. Chem. Phys.* **2000**, *2*, 2067−2073.
(105) Gdanitz, R. J.; Ahlrichs, R. *Chem. Phys. Lett.* **1988**, *143*, 413−420.
(106) Gdanitz, R. *J. Int. J. Quant. Chem.* **2001**, *85*, 281−300.
(107) Szalay, P. G.; Bartlett, R. *J. Chem. Phys. Lett.* **1993**, *214*, 481−488.
(108) Angeli, C.; Cimiraglia, R.; Evangelisti, S.; Leininger, T.; Malrieu, J. P. *J. Chem. Phys.* **2001**, *114*, 10252−10264.
(109) Angeli, C.; Cimiraglia, R.; Malrieu, J. P. *J. Chem. Phys.* **2002**, *117*, 9138−9153.
(110) Angeli, C.; Pastore, M.; Cimiraglia, R. *Theor. Chem. Acc.* **2007**, *117*, 743−754.
(111) Schapiro, I.; Sivalingam, K.; Neese, F. *J. Chem. Theory Comput.* **2013**, *9*, 3567−3580.
(112) Aguirre, F.; Husband, J.; Thompson, C. J.; Stringer, K. L.; Metz, R. B. *J. Chem. Phys.* **2003**, *119*, 10194−10201.
(113) Halfen, D. T.; Ziurys, L. M. *Chem. Phys. Lett.* **2010**, *496*, 8−13.
(114) Jonas, V.; Thiel, W. *J. Chem. Phys.* **1995**, *102*, 8474−8484.
(115) Jonas, V.; Thiel, W. *J. Chem. Phys.* **1996**, *105*, 3636−3648.
(116) Frenking, G.; Wagener, T. Transition Metal Chemistry. In *Encyclopedia of Computational Chemistry*; Schleyer, P. v. R., Allinger, N. L., Clark, T., Gasteiger, J., Kollman, P. A., Schaefer III, H. F., Schreiner, P. R., Eds.; Wiley: Chichester, 1998; pp 3073−3084.
(117) Irikura, K. K. *J. Phys. Chem. Ref. Data* **2007**, *36*, 389−397.
(118) Matyus, E.; Czako, G.; Csaszar, A. G. *J. Chem. Phys.* **2009**, *130*, 134112/1−16.
(119) Husband, J.; Aguirre, F.; Ferguson, P.; Metz, R. B. *J. Chem. Phys.* **1999**, *111*, 1433−1437.
(120) Lee, T. J.; Taylor, P. R. *Int. J. Quantum Chem. Symp.* **1989**, *23*, 199−207.
(121) Lee, T. J.; Scuseria, G. E. Achieving Chemical Accuracy with Coupled-Cluster Theory. In *Quantum Mechanical Electronic Structure Calculations with Chemical Accuracy*; Langhoff, S. R., Ed.; Kluwer Academic Publishers, Dordrecht, 1995; Vol. *13*, pp 47−108.
(122) Metz, R. B.; Nicolas, C.; Ahmed, M.; Leone, S. R. *J. Chem. Phys.* **2005**, *123*, 114313/1−6.
(123) Ruscic, B.; Pinzon, P. E.; Morton, M. L.; Srinivasan, N. K.; Su, M.-C.; Sutherland, J. W.; Michael, J. V. *J. Phys. Chem. A* **2006**, *110*, 6592−6601.
(124) Moore, C. E. *Atomic Energy Levels*; NSRDS-NBS Circular No. 35; NSRDS-NBS: Washington, DC, 1971.
(125) Schulz, R. H.; Armentrout, P. B. *J. Phys. Chem.* **1993**, *97*, 596−603.
(126) Clemmer, D. E.; Chen, Y. M.; Khan, F. A.; Armentrout, P. B. *J. Phys. Chem.* **1994**, *98*, 6522−6529.
(127) Schröder, D.; Fiedler, A.; Ryan, M. F.; Schwarz, H. *J. Phys. Chem.* **1994**, *98*, 68−70.
(128) Scherlis, D. A.; Estrin, D. A. *Int. J. Quantum Chem.* **2002**, *87*, 158−166.
(129) Tzeli, D.; Mavridis, A. *J. Phys. Chem. A* **2005**, *109*, 9249−9258.
(130) Weigend, F.; Furche, F.; Ahlrichs, R. *J. Chem. Phys.* **2003**, *119*, 12753−12762.
(131) Neese, F.; Petrenko, T.; Ganyushin, D.; Olbrich, G. *Coord. Chem. Rev.* **2007**, *251*, 288−327.
(132) Wanko, M.; Hoffmann, M.; Strodel, P.; Thiel, W.; Neese, F.; Frauenheim, T.; Elstner, M. *J. Phys. Chem. B* **2005**, *109*, 3606−3615.
(133) Altun, A.; Yokoyama, S.; Morokuma, K. *J. Phys. Chem. B* **2008**, *112*, 16883−16890.
(134) Altun, A.; Yokoyama, S.; Morokuma, K. *J. Phys. Chem. A* **2009**, *113*, 11685−11692.
(135) Karlicky, F.; Otyepka, M. *J. Chem. Theory Comput.* **2011**, *7*, 2876−2885.
(136) Sakellaris, C. N.; Miliordos, E.; Mavridis, A. *J. Chem. Phys.* **2011**, *134*, 234308/1−16.
(137) Sorkin, A.; Iron, M. A.; Truhlar, D. G. *J. Chem. Theory Comput.* **2008**, *4*, 307−315.